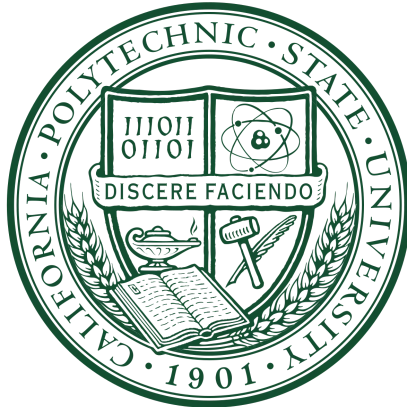


# Electroporator for the Extraction of Algae Biofuel



by

Xander Zell, Qiying Huang, Ashley Scharber, Hank Wai, and Yoel Ghebreyesus

Senior Project

ELECTRICAL ENGINEERING DEPARTMENT  
California Polytechnic State University

San Luis Obispo  
Spring 2022

## **Abstract**

Algae is a biofuel source and an eco-friendly wastewater treatment method. This report describes the development of an Electroporator [1], a Pulsed Electric Field (PEF) generator. PEF pulses (3.33MV/m to 10MV/m intensity), pulse length (5 $\mu$ s to 95 $\mu$ s), pulse period (10 $\mu$ s to 100 $\mu$ s), and number of pulses (10+) are applied to algae cells for lipid extraction. The algae sample is suspended between two conductor-coated (Indium Tin Oxide, ITO) microscope slides separated by 0.03 mm. Required field intensity range (3.33MV/m to 10MV/m) corresponds to minimum voltage range 100V to 300V.

## Table of Contents

|   |           |
|---|-----------|
| <b>Chapter 1: Introduction</b>  | <b>1</b>  |
| 1.1 Introduction  | 1         |
| 1.2 Engineering Specifications  | 2         |
| <b>Chapter 2: Electroporator Circuits</b>                                 | <b>3</b>  |
| 2.1 L0 Decomposition  | 3         |
| 2.2 L1 Decomposition  | 4         |
| 2.3 Module Function Description   | 5         |
| 2.4 Low-Side Switching Capacitive Circuit                                 | 6         |
| 2.4.1 Simulation  | 8         |
| 2.4.2 Testing   | 8         |
| 2.4.3 Summary   | 10        |
| 2.5 Bootstrapped High Side Switching Capacitive Circuit                   | 11        |
| 2.5.1 Logic Table   | 11        |
| 2.5.2 Testing   | 13        |
| 2.5.3 Summary   | 16        |
| 2.6 Inductive Circuit   | 16        |
| 2.6.1 Design Principles   | 16        |
| 2.6.2 Implementation  | 17        |
| 2.6.3 Testing   | 19        |
| 2.6.4 Conclusion  | 21        |
| 2.7 Performance Comparison  | 22        |
| <b>Chapter 3: Algae Chamber Characterization</b>                          | <b>23</b> |
| 3.1 Introduction  | 23        |
| 3.2 I-V Current-Voltage Algae Chamber Modeling                            | 25        |
| 3.2.1 Determining the Chamber Model                                       | 25        |
| 3.2.2 Passive Component Value Calculations for Chamber Model              | 28        |
| 3.3 Algae Chamber I-V Model vs. Algae Species                             | 31        |
| 3.3.1 ITO Glass Slides  | 36        |
| 3.4 Results   | 37        |
| 3.5 Discussion  | 39        |
| <b>Chapter 4: Algae Classification Using Convolutional Neural Network</b> | <b>40</b> |
| 4.1 Introduction  | 40        |
| 4.1.1 Goal  | 40        |
| 4.1.2 Background and Methods  | 40        |
| 4.2 Algae Species Information   | 41        |
| 4.2.1 Algae Strains   | 41        |

|   |           |
|---|-----------|
| 4.2.2 Algae Image Data  | 42        |
| 4.3 Convolutional Neural Network Approach   | 43        |
| 4.3.1 YOLOv5 Object Detection Algorithm   | 43        |
| 4.3.2 Creating a Dataset of Algae Labels  | 44        |
| Algae Image Capture   | 44        |
| Algae Image Labeling  | 45        |
| 4.3.3 YOLOv5 Algorithm with coco128 Dataset                                       | 46        |
| coco128 Dataset   | 46        |
| Evaluation of YOLOv5 algorithm with coco128 dataset                               | 47        |
| 4.3.4 YOLOv5 Algorithm with custom Algae Dataset                                  | 48        |
| 4.3.5 Convolution Neural Network (CNN) Performance Evaluation                     | 50        |
| 4.3.6 Further Application   | 51        |
| <b>Chapter 5: Conclusion</b>  | <b>52</b> |
| <b>Appendix A: Arduino Pulse Code</b>   | <b>53</b> |
| <b>Appendix B: Electroporator Bills of Materials and Timeline</b>                 | <b>55</b> |
| <b>Appendix C: Background &amp; Terminology of Convolutional Neural Network</b>   | <b>60</b> |
| <b>Appendix D: Graphical User Interface (GUI) for Simplified Data Acquisition</b> | <b>64</b> |
| Agilent 33220A Arbitrary Waveform Generator GUI:                                  | 64        |
| Description:  | 64        |
| Requirements:   | 64        |
| Instructions:   | 64        |
| Agilent DSO-X 2002A Digital Storage Oscilloscope GUI:                             | 66        |
| Description:  | 66        |
| Requirements:   | 66        |
| Instructions:   | 66        |
| <b>Appendix E: Digital Multimeter Automation Script</b>                           | <b>68</b> |
| Description:  | 68        |
| Python Code:  | 68        |
| <b>Appendix F: Senior Project Analysis</b>  | <b>70</b> |
| Summary of Functional Requirements  | 70        |
| Primary Constraints   | 70        |
| Economic  | 70        |
| If manufactured on a commercial basis:  | 71        |
| Environmental   | 72        |
| Manufacturability   | 72        |

|                           |           |
|---------------------------|-----------|
| Sustainability            | 73        |
| Ethical                   | 73        |
| Health and Safety         | 74        |
| Social and Political      | 74        |
| Development               | 75        |
| <b>References</b>         | <b>76</b> |
| <b>Group Contribution</b> | <b>78</b> |

## Chapter 1: Introduction

### 1.1 Introduction

Efforts to establish a sustainable ecosystem and reduce carbon emissions have become increasingly valuable. The effects of fossil fuels on the environment further catalyze a call for change, one in particular being the replacement of non-renewable fuel sources with sustainable biofuels to achieve carbon neutrality. Biofuels produced from microalgal biomass have received growing recognition as promising alternatives to conventional petroleum-derived fuels [1].

Microalgal cell pretreatment procedures must be considered prior to subsequent lipid extraction due to rigidity of algae cell wall structure. Some commonly used pretreatment methods are: 2,450-MHz Microwave-assisted extraction [2], Ultrasonication extraction[3], Chemical Methods [4], and Enzymic Disruption [5], etc. These methods are difficult to scale, costly, and include challenges to maintaining environmental sustainability. Electroporation is a promising cell disruption method as it requires simple equipment and operating procedures with high energy efficiency [6].

Electroporation is the process of applying Pulsed Electric Field (PEFs) to algae cells. PEFs are microsecond-range voltage discharge pulses that rupture (lyse) cell membranes' phospholipid bilayers, creating reversible aqueous pores to release their lipid-rich contents. Electrical potentials of 0.5-1V established across opposite poles of a cell drives charged molecules (lipids) through the pores [7].

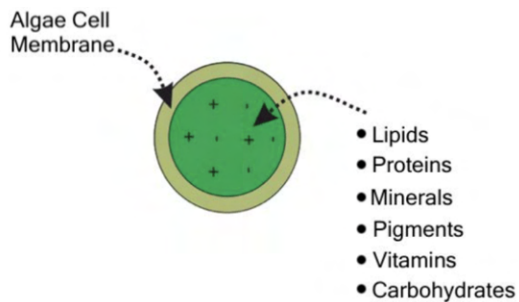


Fig. 1.1: Algae Cell Interior [2]

The previous Electroporator circuit design [8] exhibits an 80% input-to-output voltage drop due to 250  $\mu$ s rise time of Solid-State Relays (SSR, G3VM-20CR), which exceed the desired pulse duration (5  $\mu$ s - 100  $\mu$ s). In our design, Gallium Nitride MOSFETs (GaNFETs) replace SSRs. The TPH3208PS GaNFET switches in nanoseconds ( $t_{rise} = 8\text{ns}$ , and  $t_{fall} = 7\text{ns}$ , less than 1% of the intended pulse duration) and is rated for  $V_{DS} < 650\text{V}_{DC}$ .

This project proposes a new system which operates in three stages: (1) Storage capacitor charging, (2) Pulse delivery across algae chambers, and (3) Post-treatment algae sample analysis. In stage 1, the Trek 601C voltage amplifier generates 100-300 V<sub>DC</sub> (limited 10mA I<sub>DC</sub>) to charge

the storage capacitor. An Agilent 33220A Waveform generator (set to DC output mode, 2-6V<sub>DC</sub>) controls the Trek 601C DC Amplifier with 50x amplification factor. In stage 2, the pulsing circuit converts the storage capacitor's energy to electric field pulses across the algae chamber. In stage 3, an image recognition algorithm records algae microscope images or videos and extracts algae lysis information (See Chapter 4 for more information).

## 1.2 Engineering Specifications

*TABLE I-1*  
ENGINEERING SPECIFICATION

| Spec Number | Parameter                | Target (units) | Tolerance | Risk (H, M, L) | Compliance (A, T, S, I) |
|-------------|--------------------------|----------------|-----------|----------------|-------------------------|
| 1           | Pulse width              | 5 µs - 100 µs  | ± 1%      | L              | A, T                    |
| 2           | Number of Pulses         | 1 - 100        | -         | L              | A, T                    |
| 3           | Pulse voltage            | 100 - 300 V    | ± 1%      | H              | A, T                    |
| 4           | Electric Field Strength  | 25 - 50 kV/cm  | ± 1%      | H              | A, T                    |
| 5           | Source AC Power          | 120 V AC       | -         | M              | T                       |
| 6           | Temperature during tests | 25 C           | -         | L              | T                       |

## Chapter 2: Electroporator Circuits

### 2.1 L0 Decomposition

The electroporator circuit applies PEF treatment to algae samples using fast-switching GaNFETs. Fig. 2 is the system Level 0 Block Diagram.

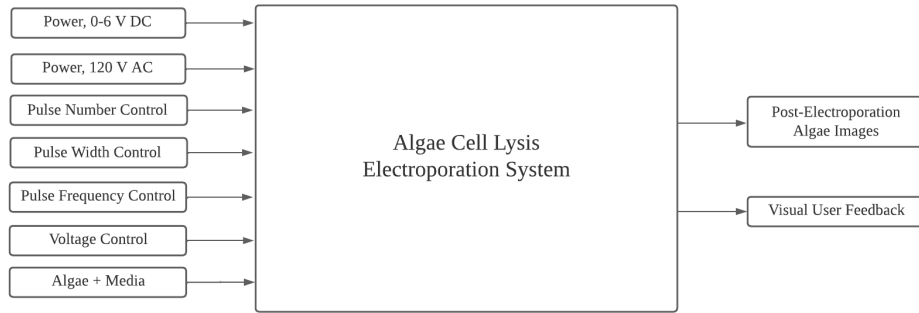


Fig. 2-1. L0 Decomposition Black Box Diagram

## 2.2 L1 Decomposition

Fig. 2-2 describes the level 1 block diagram of the low-side capacitive switching electroporator circuit. Table 2-1 contains detailed descriptions of each block.

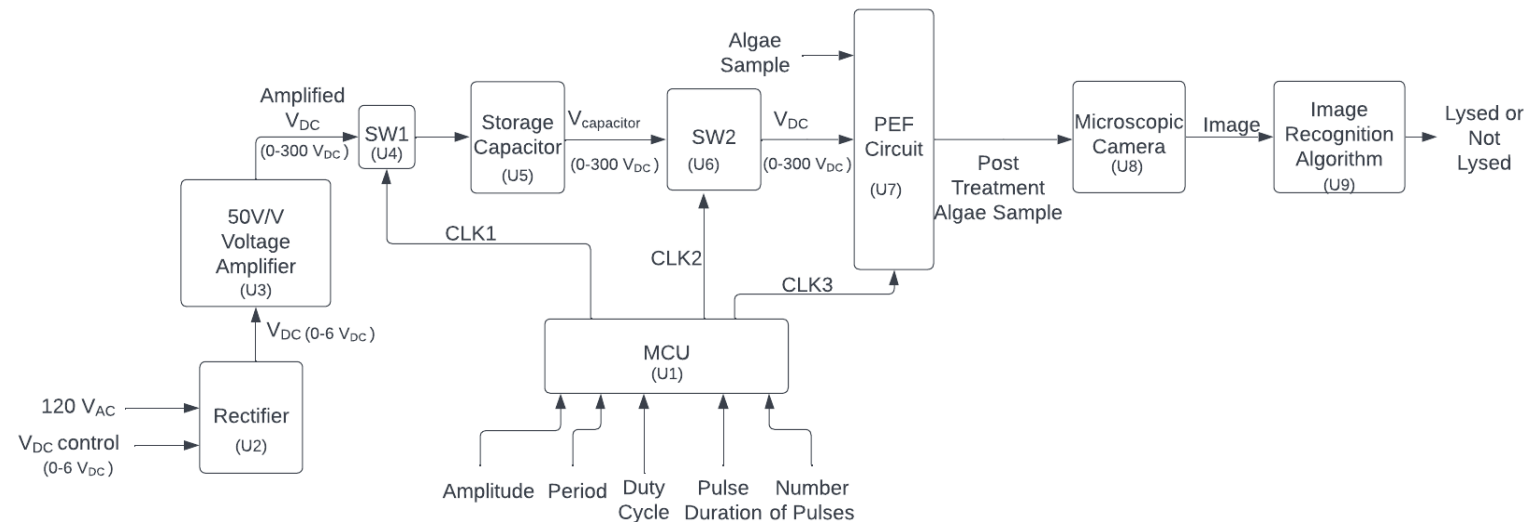


Fig. 2-2. Capacitive Circuit L1 Decomposition Black Box Diagram

## 2.3 Module Function Description

*TABLE 2-1*  
MODULE FUNCTION DESCRIPTION

| <i>Module</i>                                    | <i>Inputs</i>  | <i>Outputs</i>   | <i>Functionality</i>  |
|--|--|--|---|
| <b>Electroporator System (Level 0 Black Box)</b> | Algae Sample: 5 $\mu$ L<br>Input: 120 VAC<br>Settings: Pulse width (4.877 $\mu$ s-100 $\mu$ s) based on min write time, Pulse voltage (200-500V) | Lysed Algae/Intracellular Contents, 5 $\mu$ L with medium<br>Information: Display operation success or failure | Lyse (break) the cell membrane of algae cells to release lipids used in biofuel production. Provide pulse feedback to confirm successful lysing.  |
| <b>U1 MCU</b>                                    | Desired pulse parameters(amplitude, duty cycle, period, length of pulse train)   | Control signals to switch 1, switch 2, and the PEF pulsing circuit   | Generate timing signals to control the charging and discharging of the storage capacitor.<br>Generate timing signals to control the GaNFETs inside the PEF circuit to deliver desired pulses across the algae chamber |
| <b>U2 Rectifier</b>                              | 120V <sub>AC</sub><br>V <sub>DC</sub> Parameter  | 0-6 V <sub>DC</sub>  | Convert AC voltage to DC voltage  |
| <b>U3 Amplifier</b>                              | 2-6 V <sub>DC</sub>  | 100-300 V <sub>DC</sub> , 0-10mA   | Amplify Low Voltage DC into High Voltage DC (50V/V)   |
| <b>U4 SW1</b>                                    | MCU CLK1 (5 V <sub>DC</sub> )<br>100 - 300 V <sub>DC</sub> from U3   | ON: 100-300 V <sub>DC</sub><br>OFF: 0 V <sub>DC</sub>  | Protect the rectifier and amplifier from possible damages caused by current overdrawn   |
| <b>U5 Storage Capacitor</b>                      | 100 - 300 V <sub>DC</sub>  | Up to 300 V <sub>DC</sub>  | Store DC voltage to generate electric field pulses across the algae chamber.  |
| <b>U6 SW2</b>                                    | MCU CLK2 (5 V <sub>DC</sub> )<br>0-300 V <sub>DC</sub> from the storage capacitor  | ON: 100-300 V <sub>DC</sub> from the storage capacitor<br>OFF: 0 V <sub>DC</sub>                               | Release energy (100-300 V <sub>DC</sub> ) from storage capacitor  |
| <b>U7 PEF Circuit</b>                            | 5 $\mu$ L Algae Cells<br>0-300 V <sub>DC</sub> power from U5<br>MCU CLK3 (5 V <sub>DC</sub> )  | 100-300 V <sub>square</sub> by the capacitor circuit   | Apply voltage pulses to generate an electric field across the chamber to lyse the cell wall and cell membrane of the algae. The necessary Field strength is ~4.7 V/ $\mu$ m.  |
| <b>U8 Microscope Camera</b>                      | Post Treatment Algae Sample  | Microscope Image   | Provide image information for the image recognition algorithm to conduct analysis   |
| <b>U9 Image Recognition Algorithm</b>            | Pre-pulse and Post-pulse of 640 by 480 pixels<br>BMP, TIFF algae microscope images or AVI videos @ 60fps   | Off-line or Real-Time Algae Classification (Algae Species and Location).<br>Percent Algae Lysed.               | Visualizes the movement of algae, automatically determines success of algae lysis, and provides a percentage of lysed algae if lysis is successful.   |

Initially, two circuits were considered: a capacitor bank with solid-state relays and an inductor-based circuit. The capacitive circuit charges a  $560\mu\text{F}$  capacitor from a 50x DC Voltage Amplifier, then transfers the stored energy to GaNFET-based switching circuits. The first capacitive circuit was the Bootstrapped high-side circuit, which uses three GaNFETs to switch the chamber voltage. However, the three-FET design exhibited instability. A revised low-side switching circuit is discussed in section 2.4. Alternatively, the inductive electroporator uses a low-voltage power supply and an inductor to create narrow high-voltage (70-200V) pulses. However, in testing, these pulses proved too narrow to effectively lyse algae. Details of the inductor design and testing are included in section 2.6.

## 2.4 Low-Side Switching Capacitive Circuit

The low-side circuit includes two stages: storage capacitor charging and pulse application across the chamber (Fig 2-3). An Arduino produces clock signals (CLK1-CLK4) to control circuit timing. To charge the capacitor, the user sets a DC voltage on the function generator. When CLK1 goes High, the DC Amplifier charges  $C_1$  to 50x the set voltage. This requires 50.4 seconds ( $3\tau = 3 R_1 C_1$ ). After  $C_1$  charges,  $S_1$  turns off to protect the power supply and  $S_2$  powers the pulsing circuit.  $U_1$  controls the voltage across the algae chamber. CLK3 controls pulse train period, duty cycle, and length using Arduino code parameters. When CLK3 turns  $U_1$  on, the algae chamber is charged by  $C_1$  (creating a high voltage pulse). When CLK3 is low,  $U_1$  is off and the chamber discharges. Table 3 summarizes circuit logic.

When  $U_1$  is off, the chamber stores voltage and cannot discharge. Therefore,  $R_6$  is a discharge resistor added to provide a discharging path for the algae chamber during the pulsing stage. The chamber holding voltage indicates a series capacitance (400 pF) should be included in the model. Series chamber capacitance also causes notable simulation errors – simulations showed no switching with previous chamber models (see [8] for model) because the model contained 1.1nF series capacitance that stored the voltage instead of switching. This is why we initially used the bootstrapped high-side circuit.

$R_7$  and  $U_2$  form the discharge circuit.  $C_1$  requires a minute to discharge fully through the chamber; this would discharge the chamber with every pulse train. Therefore, to safely handle  $C_1$ , it is discharged through  $R_7$  when testing is complete. For multiple tests, the capacitor remains charged to conserve power. The circuit charging and discharging time depend on the RC time constant. ( $\tau_{charging} = 3 R_1 C_1$  and  $\tau_{discharging} = 3 R_7 C_2$ )

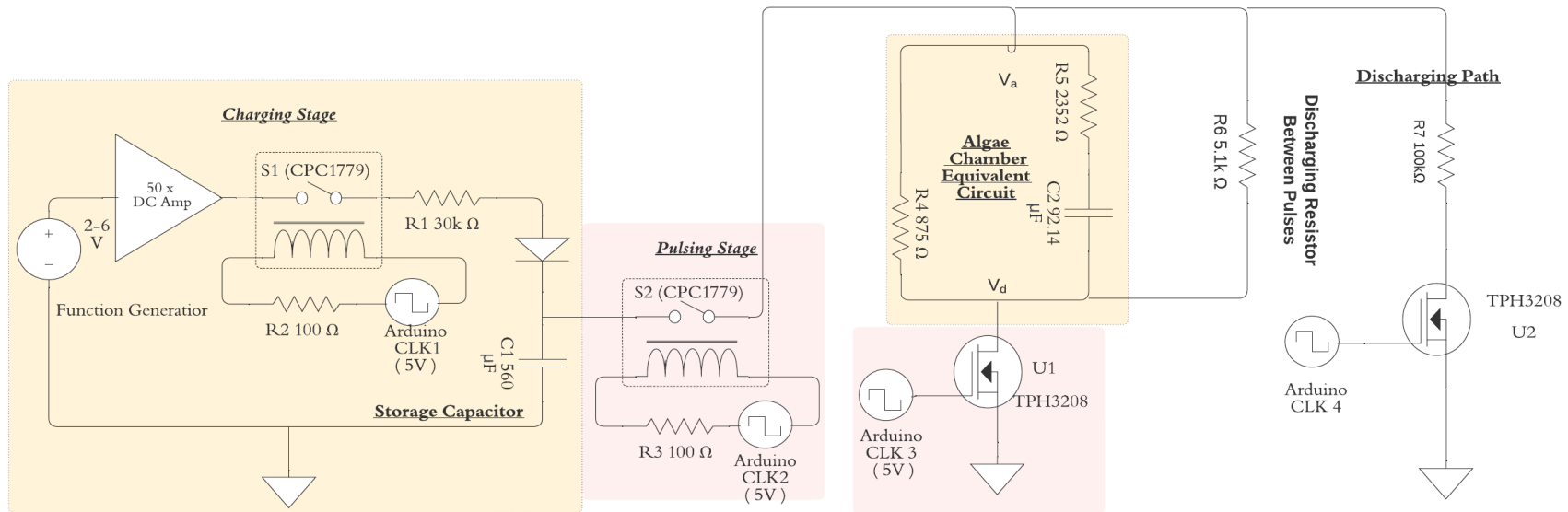


Fig 2-3. Low Side Switching Capacitive Circuit Diagram

TABLE 2-2  
LOGIC STATES; LOW SIDE SWITCHING CAPACITIVE CIRCUIT

Capacitive Electroporator Circuit Logic Table

| Case | S1  | S2  | U1  | U2  | Function   | Stage                   | Duration               |
|------|-----|-----|-----|-----|--|-------------------------|------------------------|
| 1    | ON  | OFF | OFF | OFF | Charges $C_1$                                      | Charging $C_1$          | 50s                    |
| 2    | OFF | ON  | ON  | OFF | Discharges $C_1$ + Set the voltage high across the | Pulsing Stage -High     | Min: 5µs<br>Max: 100µs |
| 3    | OFF | ON  | OFF | OFF | Discharges $C_1$ + Set the voltage low across the  | Pulsing Stage -Low      | Min: 5µs<br>Max: 150µs |
| 4    | OFF | ON  | OFF | ON  | Discharges $C_1$ + Discharges chamber              | Discharging $C_1 + C_2$ | 3 min                  |

## 2.4.1 Simulation

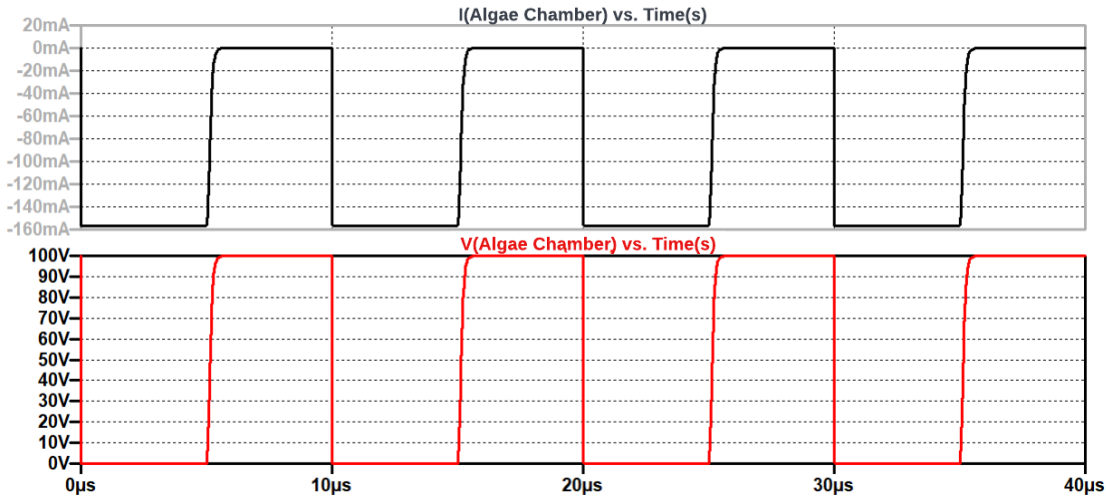


Fig. 2-4. Low Side Switching Capacitive Circuit LTSpice Simulation

## 2.4.2 Testing

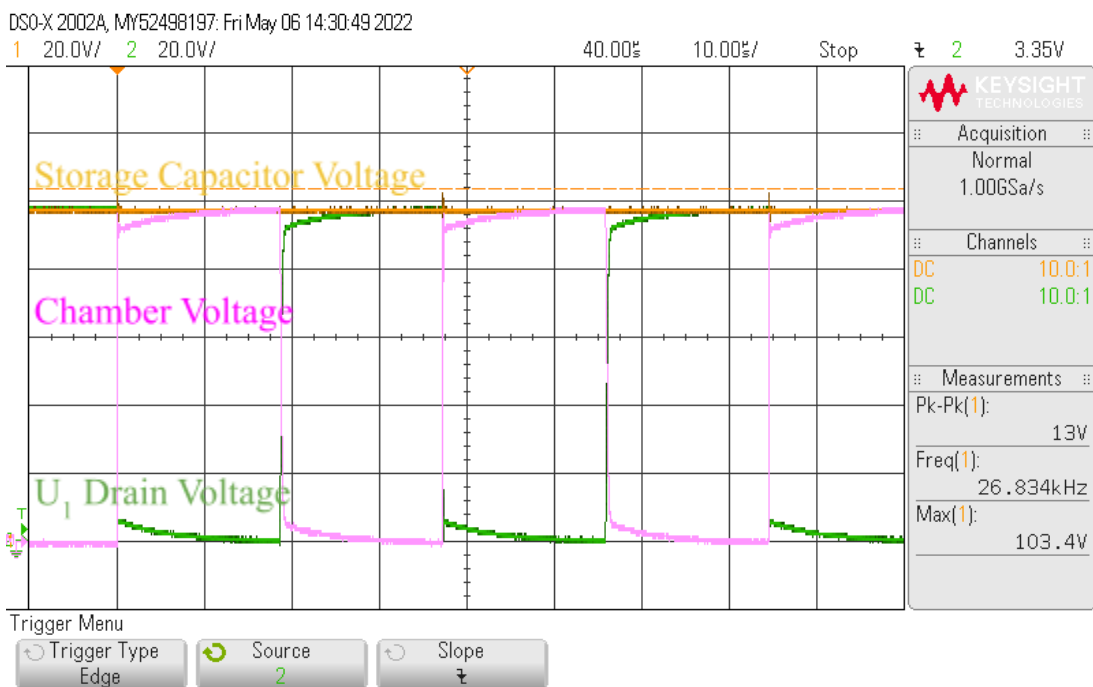


Fig 2-5. Measured Capacitor circuit chamber output ( $V_a - V_d$ ) : 100 V peak-peak, 37 us period.

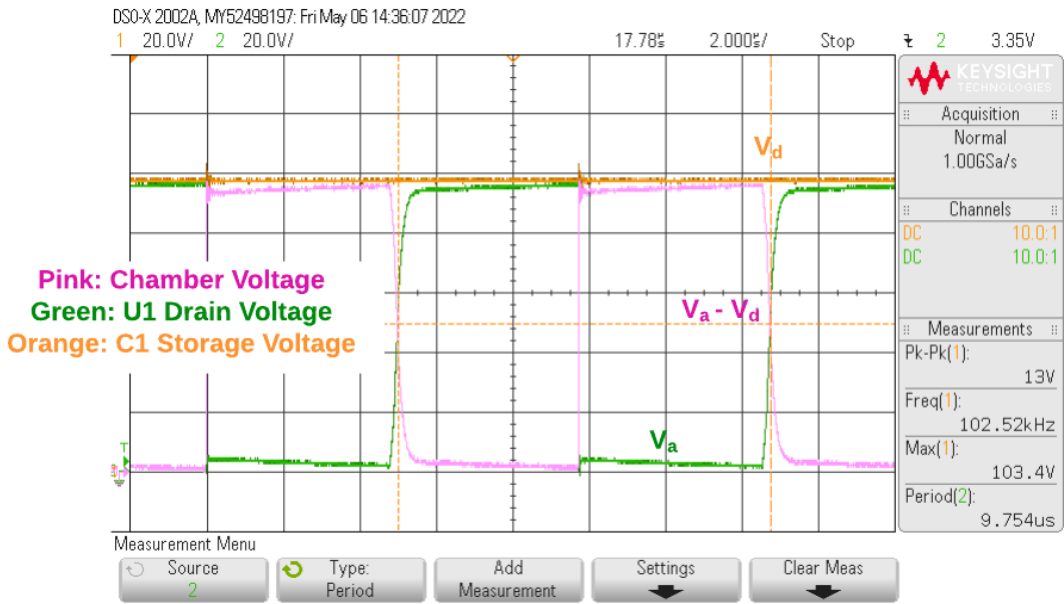


Fig. 2-6. Capacitor Maximum Switching Frequency

Removing all time delay commands from Arduino control code creates a maximum switching frequency: 102.52 kHz (50% duty cycle).

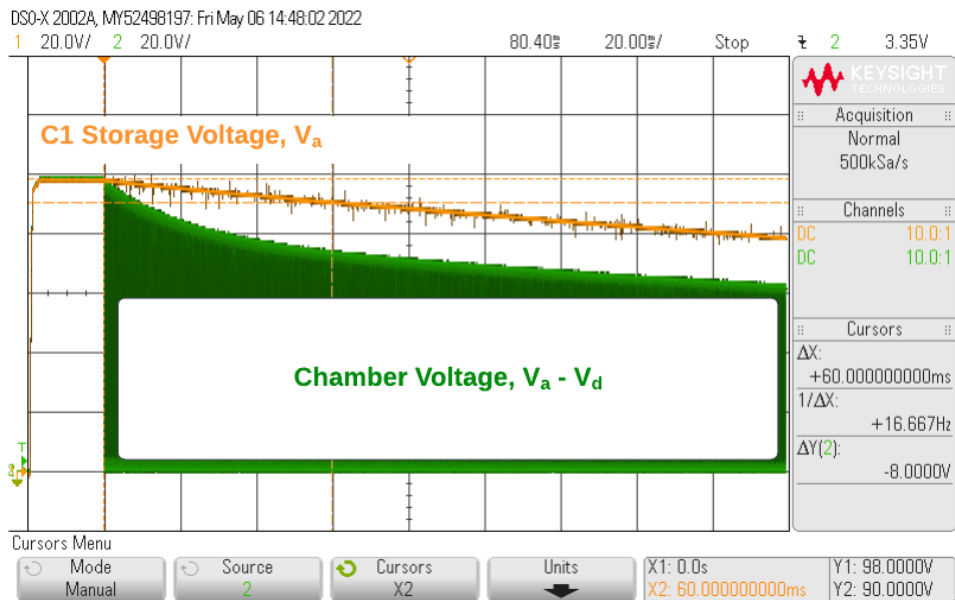


Fig. 2-7. Capacitor Discharge: 90% of initial charge at 60 ms

### **2.4.3 Summary**

The Low-side switching circuit meets all engineering specifications (Table 2-2) when tested on model loads and algae. Pulse voltage maximum is 300V, limited by component power consumption and the Trek 601C current rating limit. Using 2W resistor increases the voltage limit, and the scope capture is not necessary for lysing attempts. The minimum pulse length ( $5\mu s$ ) could be decreased using a faster microcontroller and smaller  $R_6$ . This circuit meets all the standards in Table 1-1; section 3-4 discusses our attempts to lyse algae. Section 2.5 and 2.6 discuss the inductor and high-side bootstrapping circuit, including the errors with those circuits and how our results influenced the Low-side switching circuit.

## 2.5 Bootstrapped High Side Switching Capacitive Circuit

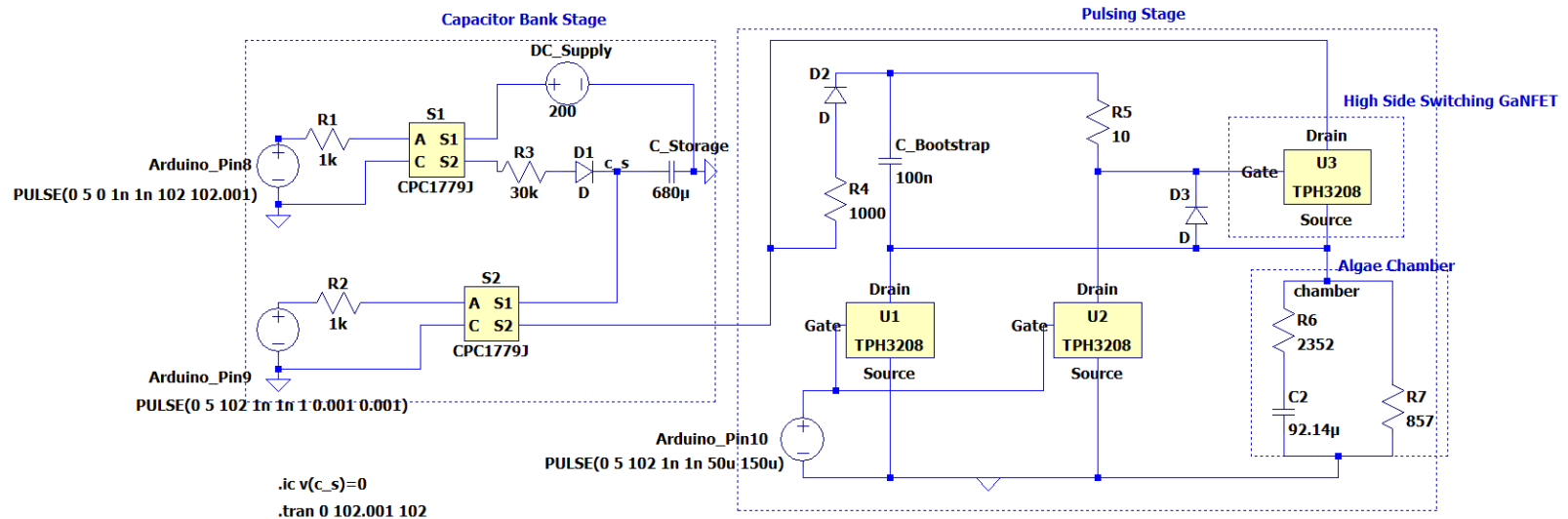


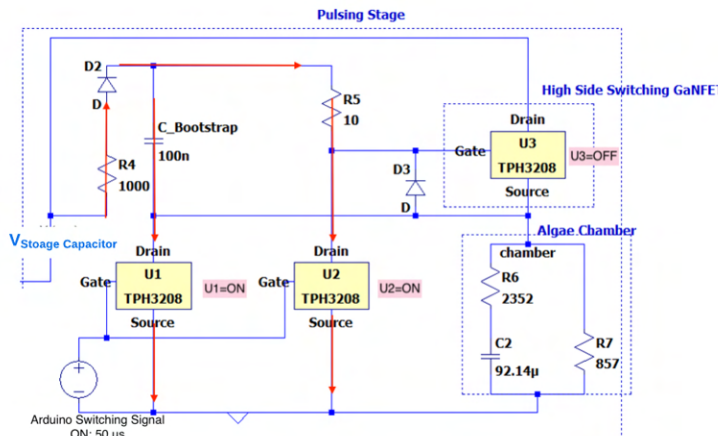
Fig. 2-8. Bootstrapped Capacitive Electroporator

### 2.5.1 Logic Table

TABLE 2-3  
LOGIC STATES; BOOTSTRAPPED HIGH SIDE SWITCHING CAPACITIVE CIRCUIT

| Case | S1  | S2  | U1  | U2  | U3  | Function                                      | Stage             | Duration                |
|------|-----|-----|-----|-----|-----|---|-------------------|-------------------------|
| 1    | ON  | OFF | OFF | OFF | OFF | Charge C_storage                              | Charging Stage    | 102 seconds             |
| 2    | OFF | ON  | ON  | ON  | OFF | Discharge C_storage,<br>Charge C_Bootstrap    | Discharge Chamber | Min: 10μs<br>Max: 100μs |
| 3    | OFF | ON  | OFF | OFF | ON  | Discharge C_storage,<br>Discharge C_Bootstrap | Charge Chamber    | Min: 3μs<br>Max: 150μs  |

Case 2: Discharge C<sub>storage</sub>, Charge C<sub>Bootstrap</sub>.  
Low Chamber Voltage



Case 3: Discharge C<sub>storage</sub>, Discharge C<sub>Bootstrap</sub>.  
High Chamber Voltage

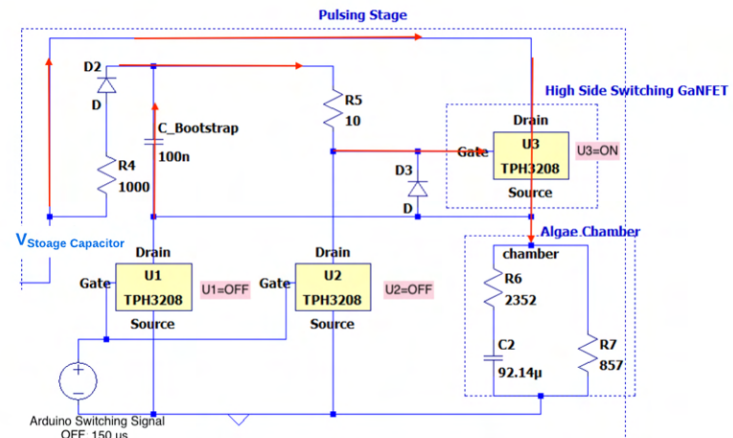


Fig. 2-9. Current Flow; Bootstrapped Electroporator Circuit

Similar to the low-side circuit, the bootstrapped electroporator includes two stages: storage capacitor charging and pulse application (Fig. 2-9). S<sub>1</sub> and S<sub>2</sub> are solid-state relays (CPC1779J). U<sub>1</sub>, U<sub>2</sub> and U<sub>3</sub> are GaNFETs (TPH3208). R<sub>3</sub> in Fig.2-8 prevents the pulsing circuit from exceeding maximum current from the power supply (Trek-601C limit 10 mA). In the capacitor charging stage, S<sub>1</sub> is “ON” to charge the storage capacitor; fully charged after 102 seconds. S<sub>1</sub> turns “OFF” and S<sub>2</sub> turns “ON”, powering the pulsing circuit.

Stage 2 is the high-side switching circuit. The load attaches to U<sub>3</sub>’s source terminal. C<sub>Bootstrap</sub> (between the gate and source of U<sub>3</sub>) provides V<sub>gs</sub> to turn “ON” U<sub>3</sub>. Figure 10 shows when the Arduino signal = 5V, U<sub>1</sub> and U<sub>2</sub> are “ON”, the bottom terminal of C<sub>Bootstrap</sub> is grounded, charging C<sub>Bootstrap</sub>. When the Arduino signal<sup>1</sup> switches to 0V, U<sub>1</sub> and U<sub>2</sub> turn off. The U<sub>3</sub> gate is no longer shorted to ground by U<sub>2</sub>, so C<sub>Bootstrap</sub> turns U<sub>3</sub> “ON”, applying voltage from C<sub>Storage</sub> to the algae chamber. In summary, the algae chamber voltage (V<sub>s</sub> at U<sub>3</sub>) is high when U<sub>1</sub> and U<sub>2</sub> are off, and low when U<sub>1</sub> and U<sub>2</sub> are on.

<sup>1</sup> Arduino signal is outputted from GPIO Pin 10

## 2.5.2 Testing

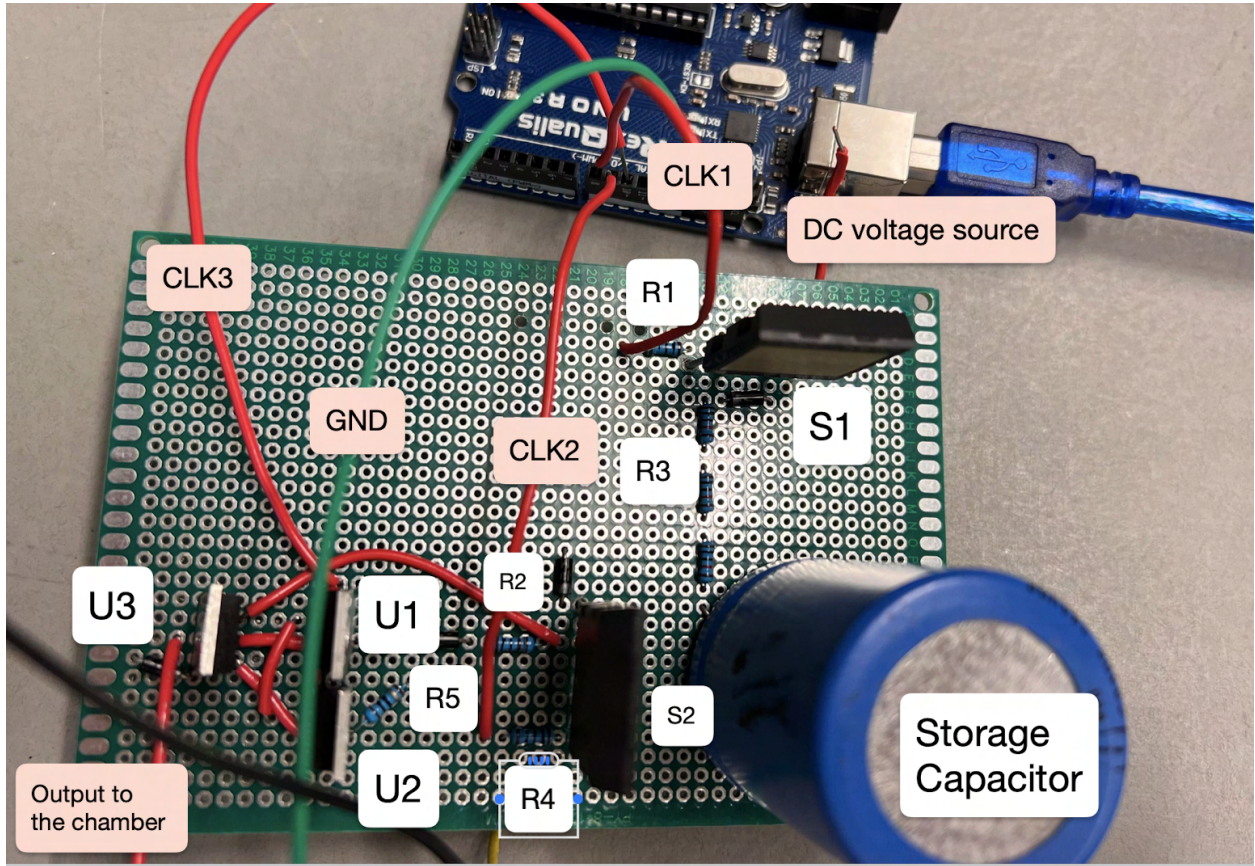


Fig. 2-10. Bootstrapped High-Side Switching Electroporator Prototype

We tested the Bootstrapped circuit using the 12V source to confirm simulated performance. Fig. 2-11 shows capacitor voltage and load voltage vs. time. These pulses are 150 $\mu$ s long because the bootstrap capacitor requires time to charge/discharge (this causes the distortion seen in Figs 2-11 and 2-12). Minimum pulse width decreases as source voltage increases because the bootstrap capacitor reaches transistor thresholds faster with greater supply voltage .

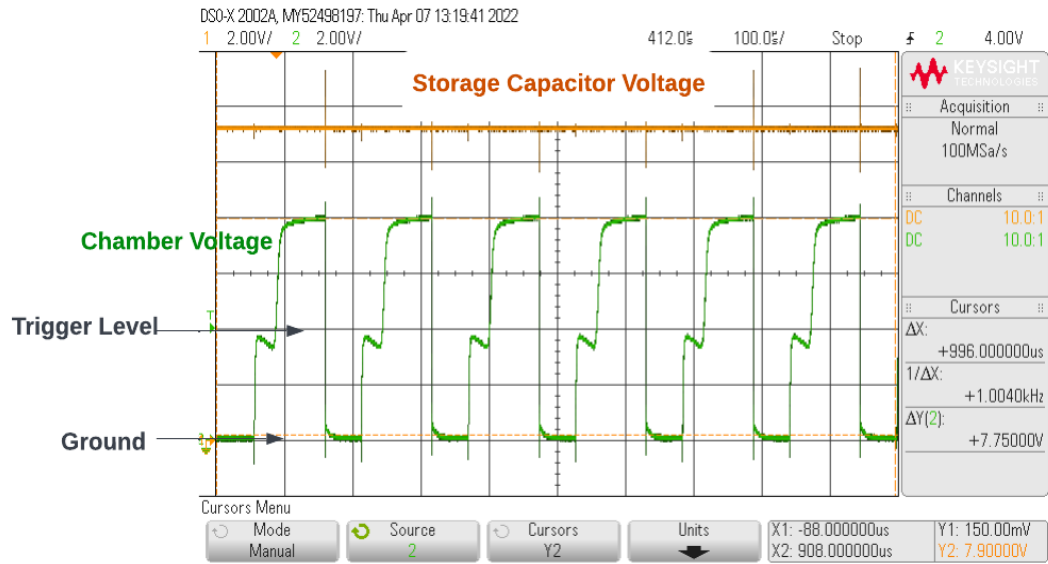


Fig. 2-11. Voltage Pulses Across Algae Chamber (12 V<sub>DC</sub>, 6.666 kHz, 67% Duty Cycle)  
Note: Green – Load Voltage, Yellow – Storage Capacitor Voltage.

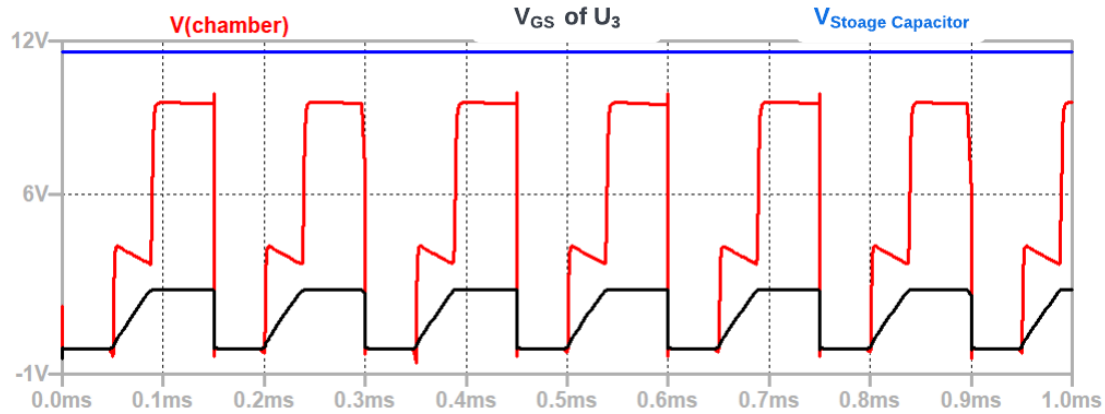


Fig. 2-12. LTSpice Pulse Simulation (12 V<sub>DC</sub>, 6.666 kHz, 67% Duty Cycle)

The waveform shape in Figs 2-11 and 2-12 are similar, but the prototype circuit peak voltage is lower than expected (Simulated V<sub>peak</sub> = 9.5V vs. Experimental V<sub>peak</sub> = 7.75V). As shown in Fig. 2-9, the 20ms delay as S<sub>2</sub> activates and diode forward bias in D1 cause this voltage drop. The waveform will look less distorted for higher storage capacitor voltage (e.g. 200V in Fig. 2-13) because U<sub>3</sub> V<sub>GS</sub> reaches V<sub>Threshold</sub> in 5 μs.

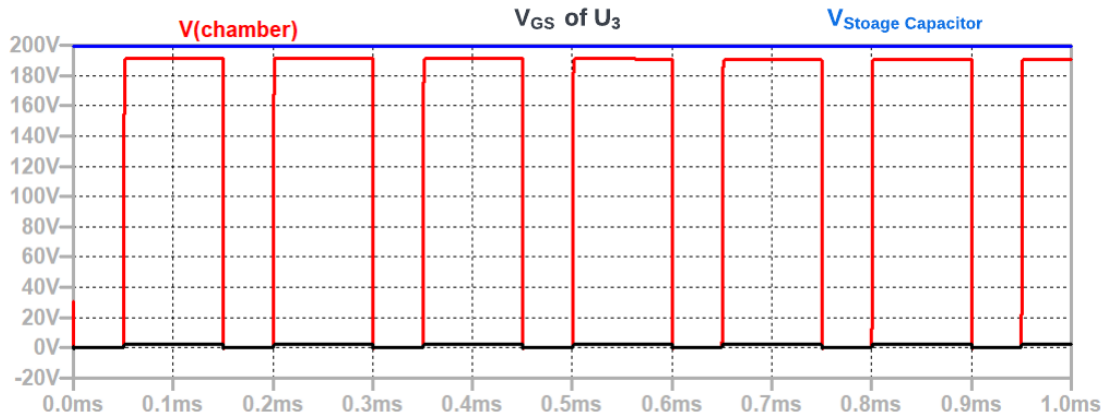


Fig. 2-13. LTSpice Pulse Simulation of Pulses across Algae Chamber (200 V<sub>DC</sub>, 6.666 kHz, 67% Duty Cycle). Greater V<sub>storage capacitor</sub> reduces distortion.

However, the delta-connected transistors create 28MHz oscillation. Around 100V, the oscillation becomes so great that the circuit is no longer able to deliver pulses with desirable parameters as shown in Fig. 2-14. High frequency voltage oscillation burns the ITO coating on the glass chamber, so this circuit design fails to lyse algae.

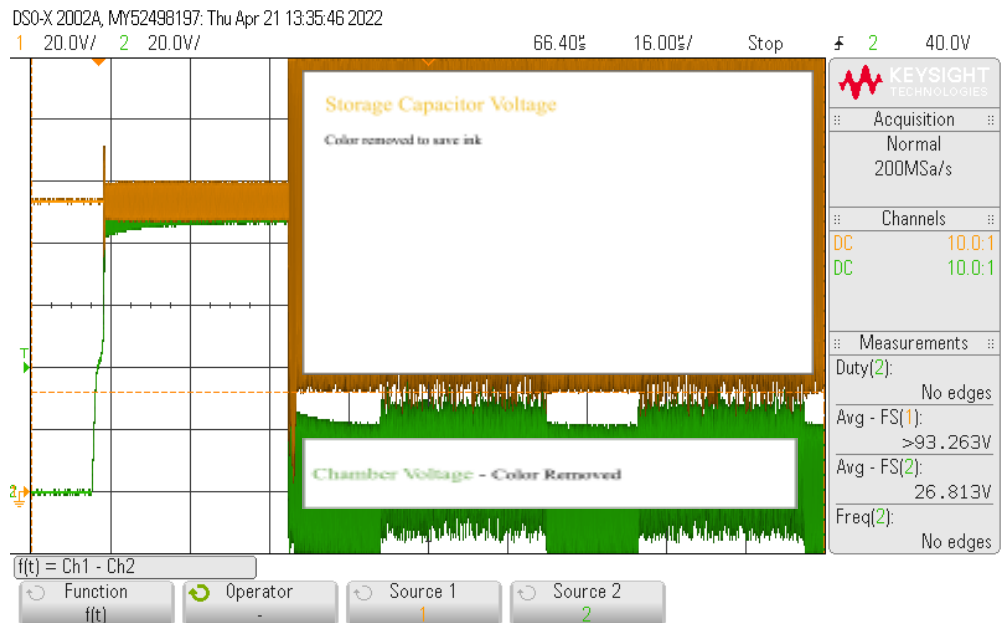


Fig. 2-14. Oscilloscope Image Algae Chamber Pulses (100 V<sub>DC</sub>, 22.2 kHz, 67% Duty Cycle)

### 2.5.3 Summary

This circuit was designed based on the original series-capacitor algae model, so the simulated circuit performance didn't match with experimental results. The bootstrapped circuit design causes catastrophic oscillations that lead to failure. With the new algae model, the low-side electroporator circuit does not require the high-side circuit, though it was useful for developing and testing the storage capacitor stage.

## 2.6 Inductive Circuit

### 2.6.1 Design Principles

The inductive electroporator uses an inductor to store current. The input current is provided by a 12 V, 2A source - the supply controls  $V_1$ , current is limited by the charging resistor  $R_1$  in Fig. 2-15. After  $L_1$  is charged, the Arduino turns  $U_1$  off.  $L_1$  current cannot change instantaneously, forcing stored current through  $R_2$  and the algae chamber. The current through  $R_2$  creates a voltage peak across  $R_2$  and the chamber. Equation 1 shows circuit period calculations based on  $L_1$ , and Equation 2 shows  $V_{\text{chamber}}$ .

$$T = L_1 \left( \frac{3}{6} + \frac{1}{R_2} \right) \approx \frac{L_1}{2} \quad (1)$$

$$V_{\text{chamber}} (\text{max}) = 0.95 \frac{V_1 R_2}{R_1} \quad (2)$$

## 2.6.2 Implementation

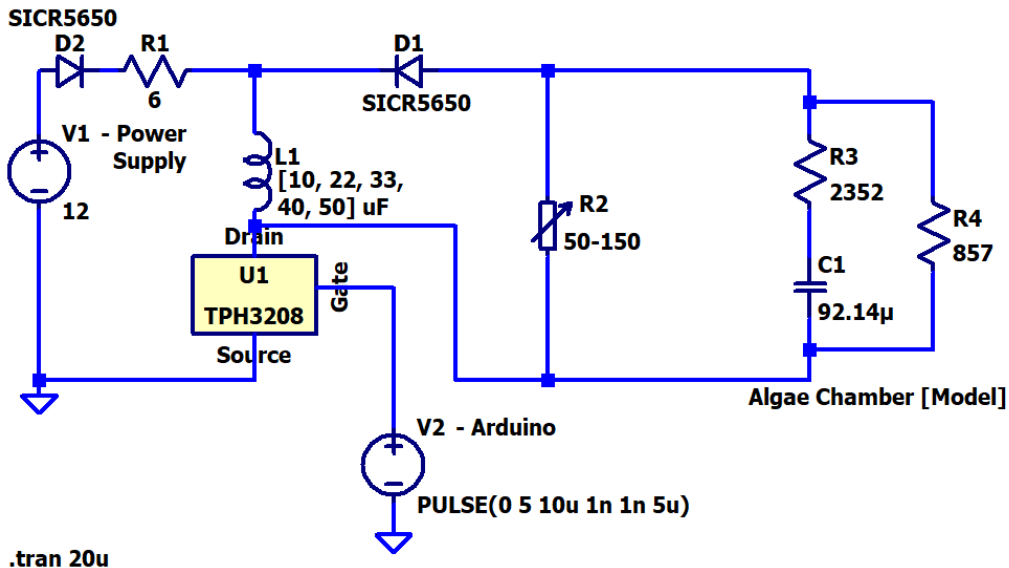


Fig. 2-15. Inductor Pulse Electric Field Generator Schematic

$R_1$  is  $6\Omega$  to maximize current from the 12V, 2A Power supply. To create a range of inductances, we use a rotary switch and five inductors ( $10, 22, 33, 40$ , and  $50 \mu H$ ). The inductance range allows the pulse periods shown in TABLE 2-4 - a range surrounding the central  $10\mu s$  period to test a range of periods. To create the variable resistor  $R_2$ , is a  $50\Omega$  resistor with a in series with  $100\Omega$  potentiometer. See Table B-2 for the full list of inductor electroporator components.

TABLE 2-4  
PULSE TRAIN PERIODS FOR SELECTED INDUCTORS

| Inductors Purchased | Period (App. A1, eq. 10) |
|---------------------|--------------------------|
| $10\mu H$           | $5.0\mu s$               |
| $22\mu H$           | $11.0\mu s$              |
| $33\mu H$           | $16.5\mu s$              |
| $40\mu H$           | $20.0\mu s$              |
| $50\mu H$           | $25.0\mu s$              |

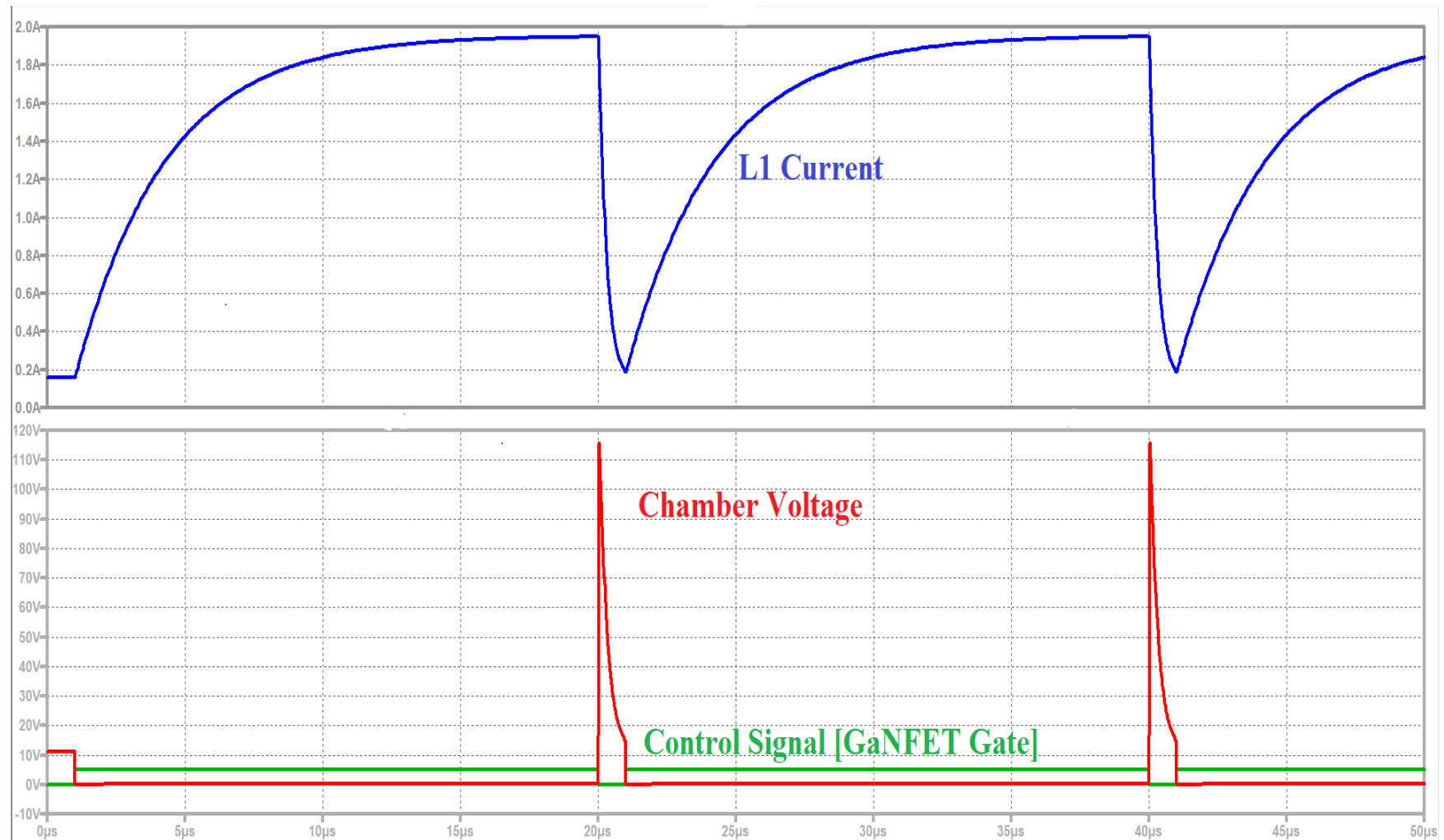


Fig. 2-16. Inductive PEF Generator LTSpice Simulation:  $V_1 = 12V$ ,  $R_1 = 6\Omega$ ,  $R_2 = 60\Omega$

### 2.6.3 Testing

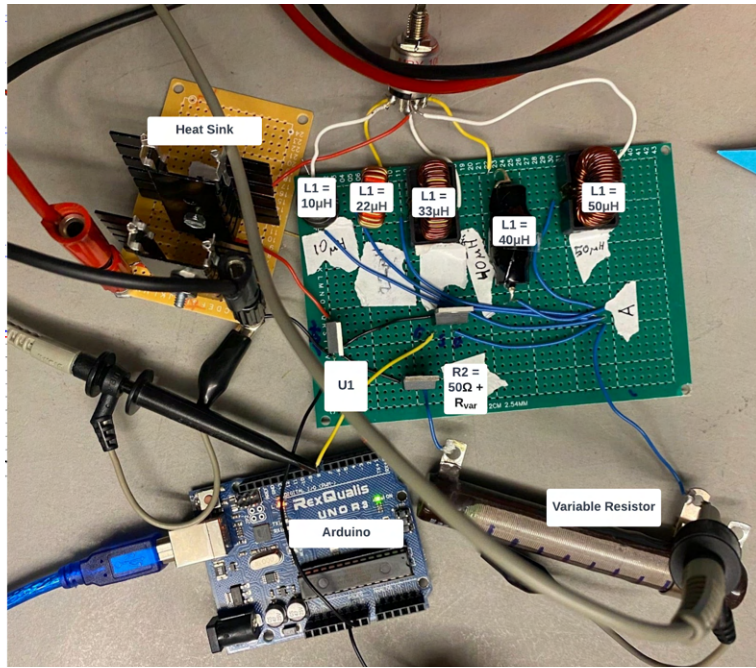


Fig. 2-17. Inductor Pulse Generator Prototype

Fig. 2-17 shows the completed inductor circuit with the Arduino in the bottom left. R<sub>1</sub> and D<sub>2</sub> are on the brown board. Variable L<sub>1</sub>, along with U<sub>1</sub>, R<sub>2</sub> and D<sub>1</sub> are on the green board. As shown in Fig. 2-17, the algae chamber is between node marked “A” and the black banana plug binding post. The heat sinks on R<sub>1</sub> and D<sub>2</sub> are necessary because R<sub>1</sub> dissipates 24W (transient).

The circuit was first tested without an algae chamber. Fig. 2-18 on the following page shows the peak generated voltage with no chamber (Here, the chamber voltage label refers to the chamber node). This proves that the circuit is capable of producing unloaded peaks over 200V unloaded. Fig. 2-19 shows example input and output voltage capture with the algae chamber connected. One substantial difference from simulations: the measured output voltage pulse [green] is less than 200ns wide, while Fig. 2-16 simulations show microsecond width pulses.

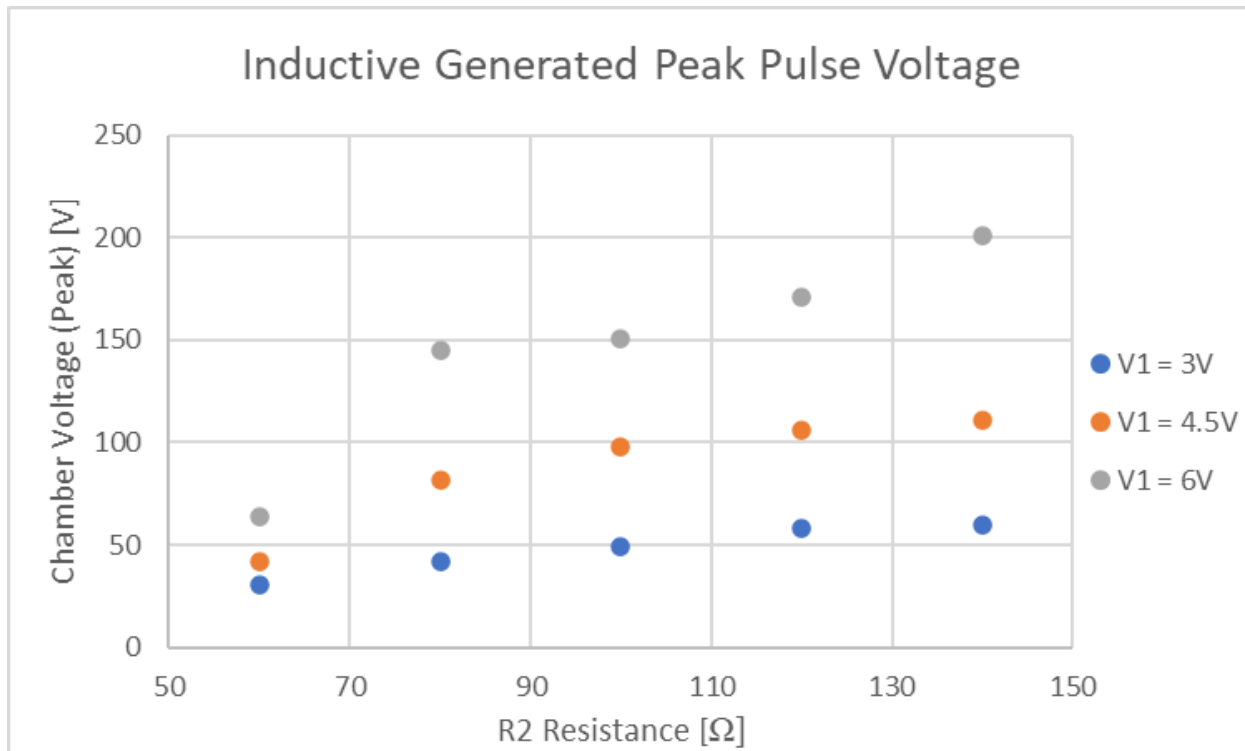


Fig. 2-18. Unloaded Peak R<sub>2</sub> Pulse Voltage [Algae Chamber is Parallel to R<sub>2</sub>]

DSO-X 2002A, MW52498197: Fri Feb 25 15:03:11 2022

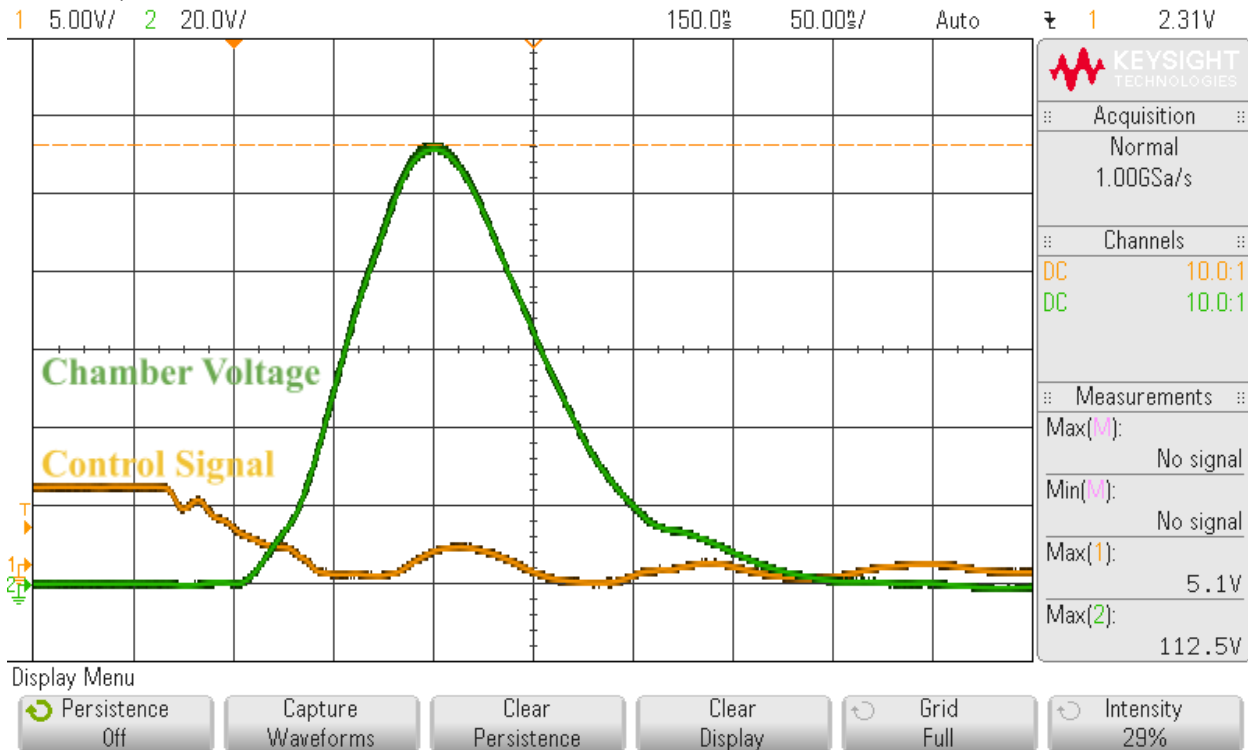


Fig. 2-19. Algae Chamber Connected Single Pulse Test, V<sub>s</sub> = 4.5V, R<sub>2</sub> = 140Ω, L = 22μH.

Fig. 2-20 shows peak output voltages when connected to the algae chamber. Compared to Fig. 2-18 unloaded pulse generator, the chamber voltage is lower because the chamber is in parallel with  $R_2$ . However, the electroporator still successfully generates peaks greater than 200V.

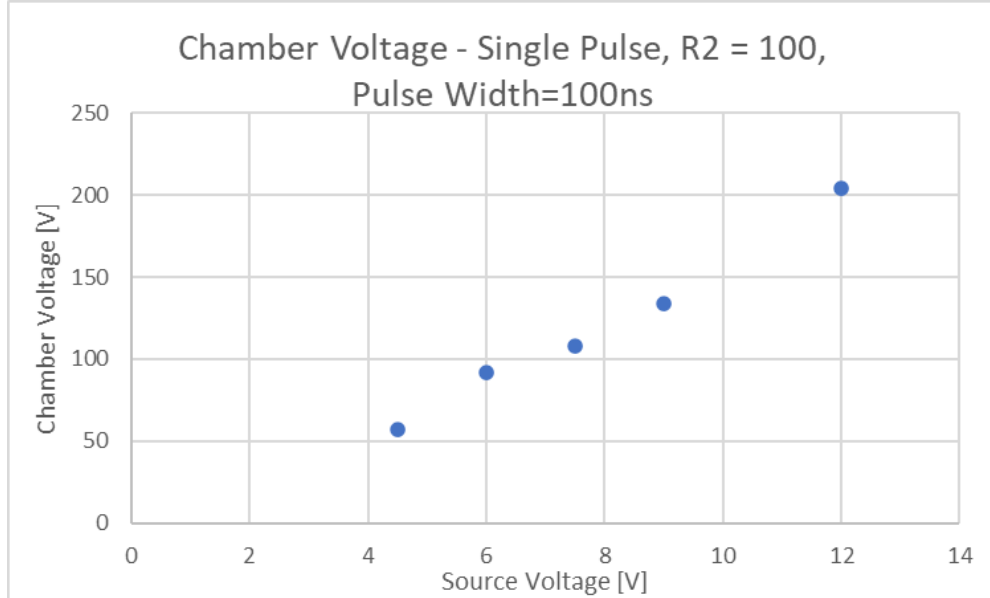


Fig. 2-20. Chamber Connected Single Voltage Pulse  $R_2 = 100$ , Pulse Width = 100 ns,  $T=20\mu s$

No algae lysis was observed when 200 V pulses applied because the duty cycle of the pulse train is too short. With the chamber attached, the pulse width decreased to approximately 100ns, for a 0.5% duty cycle. This appears too low to lyse algae. However, since the circuit uses a single inductor, the duty cycle cannot increase by changing the inductor, and changing  $R_2$  to increase duty cycle lowers chamber voltage.

## 2.6.4 Conclusion

Due to low duty cycle and inflexibility for voltage, duty cycle, and period, the inductive electroporator is currently infeasible. However, there are several avenues that could be explored to improve this circuit. First, replacing the inductor with a transformer would allow different time constants and voltages. This is commonly used in Flyback Converter DC Power supplies – Using a transformer to power additional switching circuits similar to the capacitive electroporator above could be a solution. Alternatively, using a higher-power  $V_1$  supply allows greater voltages and duty cycles. However, this device already consumes up to 24W (transient) and rapidly overheats. Both solutions improve one aspect but introduce additional performance problems.

## 2.7 Performance Comparison

TABLE 2-5  
PERFORMANCE COMPARISON

|                                       | High-Side Switching<br>Bootstrapped<br>Capacitive Circuit | Low-Side Switching<br>Capacitive Circuit | Inductive Circuit |
|---------------------------------------|---|--|-------------------|
| Variable Duty Cycle                   | ✓   | ✓  | ✗                 |
| Variable Frequency                    | ✓   | ✓  | ✓                 |
| Efficiency ( $V_{Output}/V_{Input}$ ) | 64%   | 98%                                      | *                 |
| Output Voltage Range                  | 25 Vmax   | 100V - 300V                              | 100V - 250V       |

\* $V_{out}/V_{in}$  doesn't quantifies inductor circuit efficiency -  $V_{out}$  is up to 20 times larger than  $V_{in}$ .

## Chapter 3: Algae Chamber Characterization

### 3.1 Introduction

For PEF treatment, algae samples are placed in a chamber composed of two Indium Tin Oxide (ITO) coated glass slides. Indium Tin Oxide, composed of indium (III) oxide ( $In_2O_3$ ) and tin (IV) oxide ( $SnO_2$ ), is used for biosensing due to its high electrical conductivity and optical transparency [9]. ITO slides are used because: 1) high electrical conductivity and low capacitive current apply the electromagnetic field across the algae sample instead of the glass walls, and 2) transparency allows optical microscope algae observations before and after treatment without removal from the chamber [9]. Kapton tape (an insulative film) separates the two plates by 50  $\mu m$  and limits chamber volume.

The ITO-coated slides are 25 mm wide x 25 mm long x 1.1mm thick. The glass is coated with ITO on one side (conductive side), while the opposite side is uncoated (non-conductive). Fig. 3-1 shows the algae chamber with separated slides. Chamber dimensions are shown by Table 3-1. Chambers are constructed as follows:

1. Place a Kapton tape strip on the left border of two ITO slides (conductive side)
2. Attach a metal lead on the right border of each slide using silver epoxy
3. Hold the chamber together with conductive sides facing each other. Offset chambers so that Kapton tape lies flush with the opposite conductive surface
4. Use plastic clips to clamp slides together

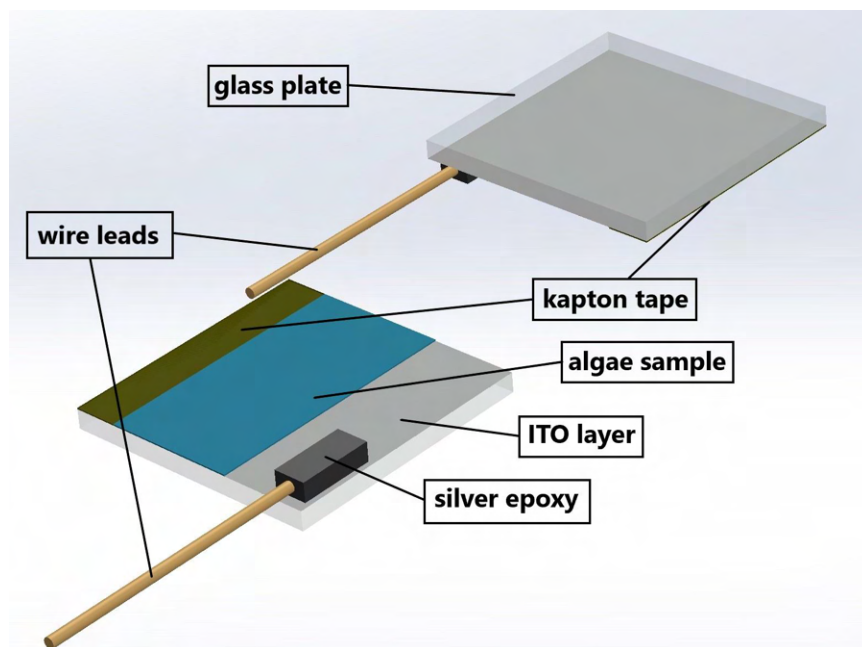


Fig. 3-1. Algae Chamber CAD Model

To use the chamber, the electroporator uses alligator clips to clamp onto the wire leads attached to the chamber using the conductive silver epoxy. Scope probes are attached at both sides of the chamber. The difference between the high-side and the low-side scope probe voltages represents algae chamber voltage. 15  $\mu\text{L}$  algae solution is inserted through the top gap using a 20  $\mu\text{L}$  pipette. Fig.3-2 shows impedance measurement circuit (Section 3.2.1) attached to the algae chamber.

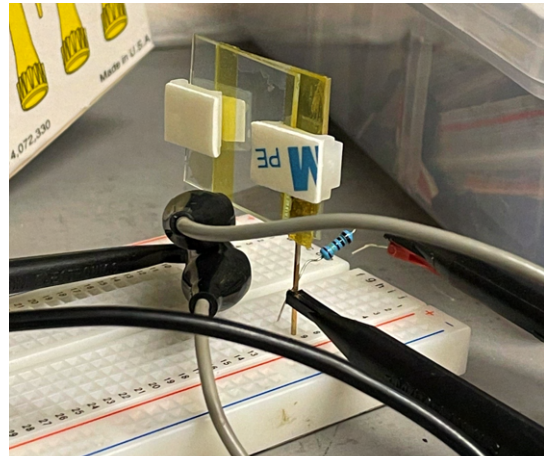


Fig. 3-2. Algae Chamber in Impedance Measuring Circuit

*TABLE 3-1*  
Algae Chamber Dimensions and Measurements

| Chamber Size Measurements  |               |                   |
|----------------------------|---------------|-------------------|
| Measurement                | Value         | Units             |
| Thickness of Glass         | 0.991 - 1.041 | mm                |
| Thickness of tape          | 51 - 151      | $\mu\text{m}$     |
| Length                     | 24            | mm                |
| Width                      | 11            | mm                |
| Area                       | 264           | (mm) <sup>2</sup> |
| Volume                     | 2.64E-08      | (m) <sup>3</sup>  |
| Volume                     | 26.40         | $\mu\text{L}$     |
| Capacitance                | 92.14         | $\mu\text{F}$     |
| Permittivity of free space | 8.854E-12     | F/m               |

Algae chamber dimensions are shown in Table 3-1 above. Using the Pittsburgh 6" Dial Precision Caliper [10], the measured ITO glass thickness is between 0.991 mm and 1.041 mm.

The ITO glass with Kapton tape attached is between 1.0922 mm and 1.143 mm. The difference between these two yields the chamber gap spacing of 51 $\mu$ m to 151  $\mu$ m.

### 3.2 I-V Current-Voltage Algae Chamber Modeling

To improve electroporator simulation accuracy, we characterize the algae chamber in terms of current-voltage relationship, steady-state behavior, and transient-mode characteristics. With this data we create a new RC model to use in design simulations. This experimental process and the required derivations to support the chamber model are described below.

#### 3.2.1 Determining the Chamber Model

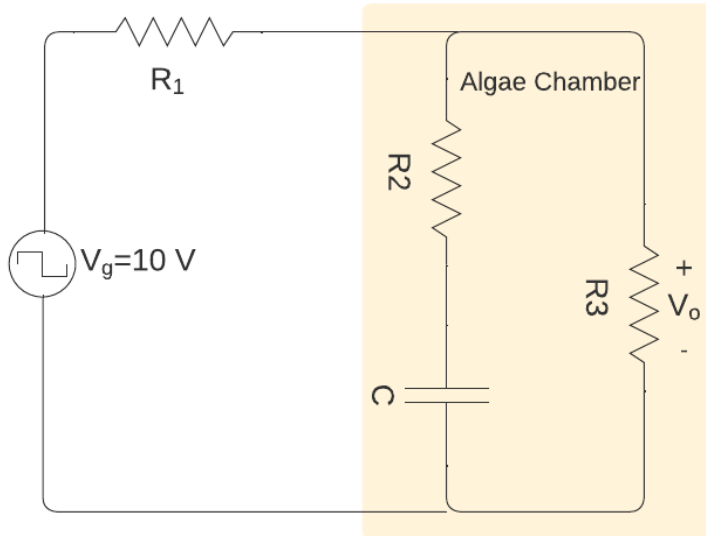


Fig. 3-3. Impedance Measurement Circuit with Proposed RC-R Model

In Fig. 3-3, the algae chamber voltage is  $V_o$ .  $R_1$  is a 1 k $\Omega$  series resistor to measure current through the algae chamber. The algae chamber impedance is defined by passive components  $R_2$ ,  $R_3$ , and  $C$ . These component values are determined by measuring chamber I-V characteristics with DC inputs and step response using a 200 mHz, 10V<sub>peak-to-peak</sub> square wave. The model of Fig 3-3 was constructed after testing the algae chamber and observing the effects of the 10V, 200 mHz step and ramp inputs.

The following conclusions were drawn after measuring the algae chamber with step and ramp inputs:

1. The equivalent resistance of the algae chamber at steady state decreases as the chamber voltage ( $V_o$ ) increases. (See Fig 3-4)
2. The algae chamber demonstrates charging characteristics since the equivalent chamber resistance after a 10V step is less than the measured resistance at steady state (Fig. 3-5)

Algae Chamber Resistance ( $R_3$ ) vs Chamber Voltage ( $V_o$ ) at 3-12 VDC Input - Desmodesmus Armatus 2/24/22

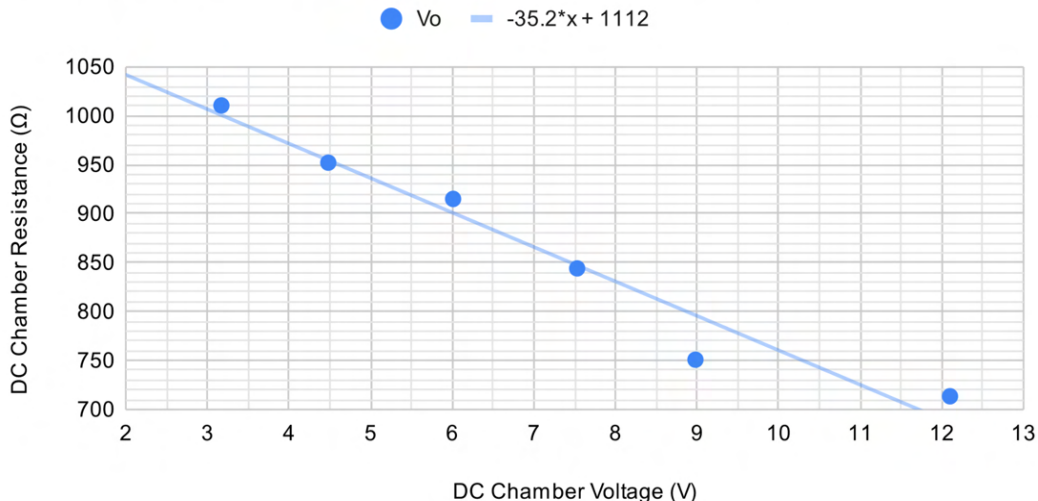


Fig. 3-4. Chamber Resistance ( $R_3$ ) vs Chamber Voltage ( $V_o$ ) (*Desmodesmus armatus* algae sample)

Fig. 3-4 represents algae chamber resistance vs.chamber voltage. The DC input ranges from 3.0 to 12 V. Equation 3-1, the Fig. 3-4 line of best fit, quantifies chamber resistance as a function of voltage.

$$\text{Algae DC impedance} = R_3 = -35.2V_o + 1112 \quad (3-1)$$

The algae chamber response to 10V step demonstrates capacitive behavior. In Fig. 3-5, when a step input is applied,  $V_o$  increases to 5.74 V at time  $t = 0+$ . The measured voltage charges to 7 V after 800 ms. Based on these observations we propose Fig. 3-3, is a RC (series  $R_2$ , C) circuit in parallel with a resistor ( $R_3$ ).

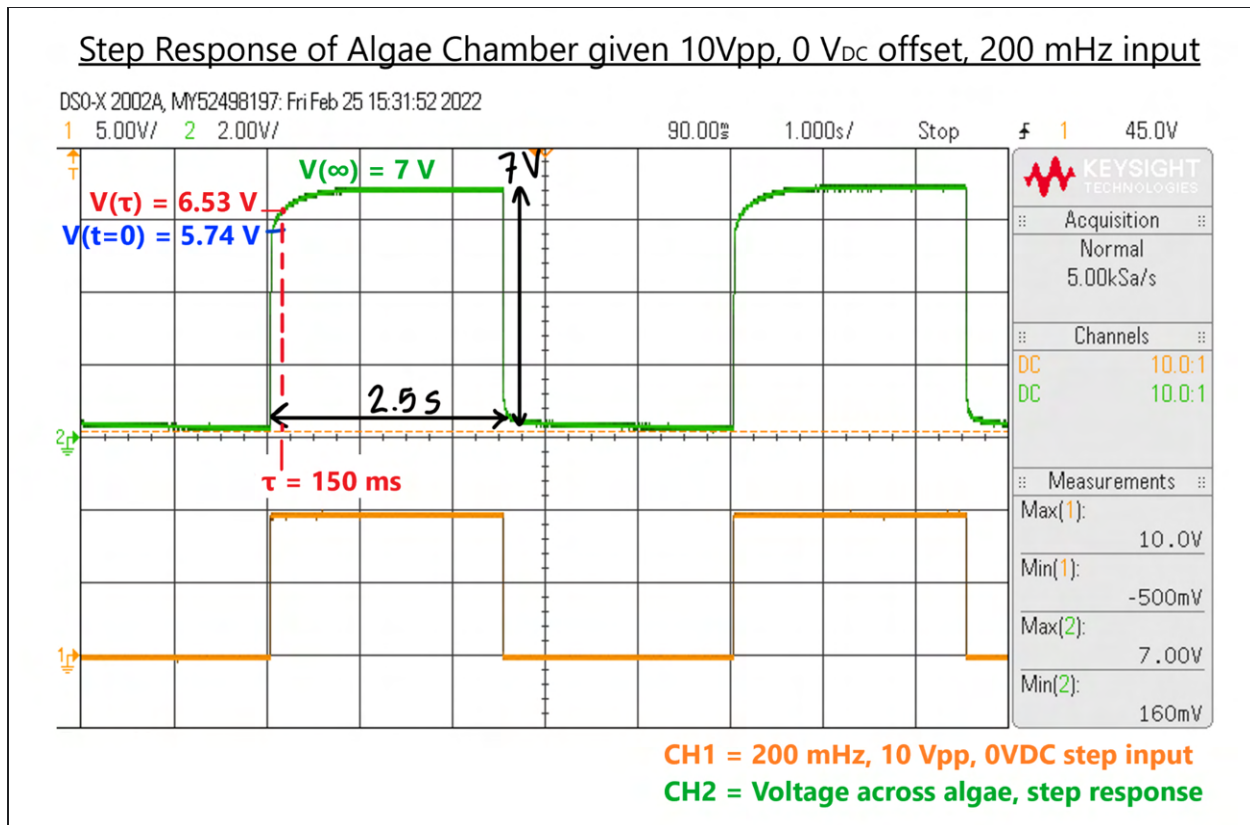


Fig. 3-5. Algae Chamber (*Desmodesmus armatus* algae) 10V Step Response. 10 Vpp, 0 V<sub>DC</sub>, 200 mHz step input

Table 3-2 represents the summary of the three different states of the algae chamber model's step response. Calculations for the passive component values and equations of the different states are completed in the following section.

*Table 3-2*  
 Algae Chamber Charging States During Step Response

| Time            | State   | Voltage                         |
|-----------------|---|---------------------------------|
| $t = 0+$        | Capacitor is <i>not</i> charged and has no initial voltage across it, and therefore acts as a short | $V_o(0) = 5.74 \text{ V}$       |
| $0 < t < 3\tau$ | Capacitor is charging   | $V(t) = 7.00 - 1.26e^{-t/\tau}$ |
| $t \geq 3\tau$  | Steady-State: Capacitor is fully charged and now functions as an open.                              | $V(t) = 7.00 \text{ V}$         |

### 3.2.2 Passive Component Value Calculations for Chamber Model

**At time t=0,** there is no voltage across the capacitor but it accepts 4.26 mA. Therefore, the capacitor initially has zero resistance. In this case, the equivalent impedance of the algae chamber is  $R_1$  in series with the parallel combination of  $R_2$  and  $R_3$ . The output voltage  $V_o$  is across the parallel combination of  $R_2$  and  $R_3$ .

$$R_{eq} = R_1 + R_2 \parallel R_3 \quad (3-3)$$

$$V_o(t = 0) = V_g \times \frac{R2 \parallel R3}{R_{eq}} \quad (3-4)$$

The voltage can be represented by the following. A is the steady-state component and B is the transient component:

$$V_o(t) = A + Be^{-t/\tau} \quad (3-5)$$

**At time t = 3τ,** the capacitor is fully charged and acts like an open. No current flows through the RC Branch. In this case, the equivalent resistance is the series combination of  $R_1$  and  $R_3$ :

$$R_{eq} = R_1 + R_3, \quad (3-6)$$

Comparing charged vs discharged states, there is a greater resistance between  $V_o$  and GND during the charged state since the capacitor is fully charged. The voltage can be represented by the following:

$$V_o(t = 3\tau) = A = 7.00 V \quad (3-7)$$

$$\text{Therefore, } B = V_o(0) - V_o(3\tau) = 5.74 V - 7.00 V = -1.26 V$$

**Between t=0 and t=3τ,** the model capacitor is charging. Eq. 3-8 gives the chamber voltage as a function of time:

$$V_o(t) = A + Be^{-t/\tau} = 7.00 - 1.26e^{-t/\tau} \quad (3-8)$$

**Finding  $R_3$ -** This is the resistance of the algae chamber at steady-state when the capacitor is fully charged. We can use equation 3-1 to solve for  $R_3$  using  $V_o = 7V$ .

$$\begin{aligned} \text{Algae impedance } &= R_3 = -35.2V_o + 1112 \\ R_3 &= -35.2(7.00) + 1112 = 856.6\Omega \end{aligned} \quad (3-9)$$

**Finding  $R_2$ -** This is the chamber impedance when the capacitor is a short (discharged). The equation for  $R_2$  is shown below:

$$\begin{aligned} V_o(0) &= A + B = 5.74V = V_g \times \frac{R_2|R_3}{R_2|R_3+R_1} \\ R_2 &= \frac{1}{\frac{V_g}{V_o(0)R_1} - \left(\frac{1}{R_3} + \frac{1}{R_1}\right)} \end{aligned} \quad (3-10)$$

Substituting  $V_g = 10\text{ V}$ ,  $V_o(0) = 5.74\text{ V}$ ,  $R_1 = 1000\Omega$ , and  $R_3 = 856.6\Omega$  in equation 3-10:

$$R_2 = 2,351.6\Omega$$

**Finding C-** To determine capacitance, we find step response voltage after one time constant.

$$\begin{aligned} V_o(t) &= 7.00 - 1.26e^{-t/\tau} \\ V_o(\tau) &= 7.00 - 1.26e^{-1} = 6.536\text{ V} \end{aligned}$$

Using Fig. 3-5, this voltage corresponds to a 150 ms time constant value, which we use to find C.

$$\begin{aligned} \tau &= 150\text{ ms} = R_{eq} \cdot C \quad (3-11) \\ R_{eq} &= R_1 + R_2 \parallel R_3 \\ R_{eq} &= 1000 + \frac{(2352)(856.6)}{(2352+856.5)} = 1,628\Omega \\ C &= \frac{\tau}{R_{eq}} = \frac{0.15}{1,628} = 92.14\mu F \end{aligned}$$

Fig. 3-6 below represents the final algae chamber model as the result of a 10 V step input. This model changes depending on algae species.

### Final Algae Chamber Model

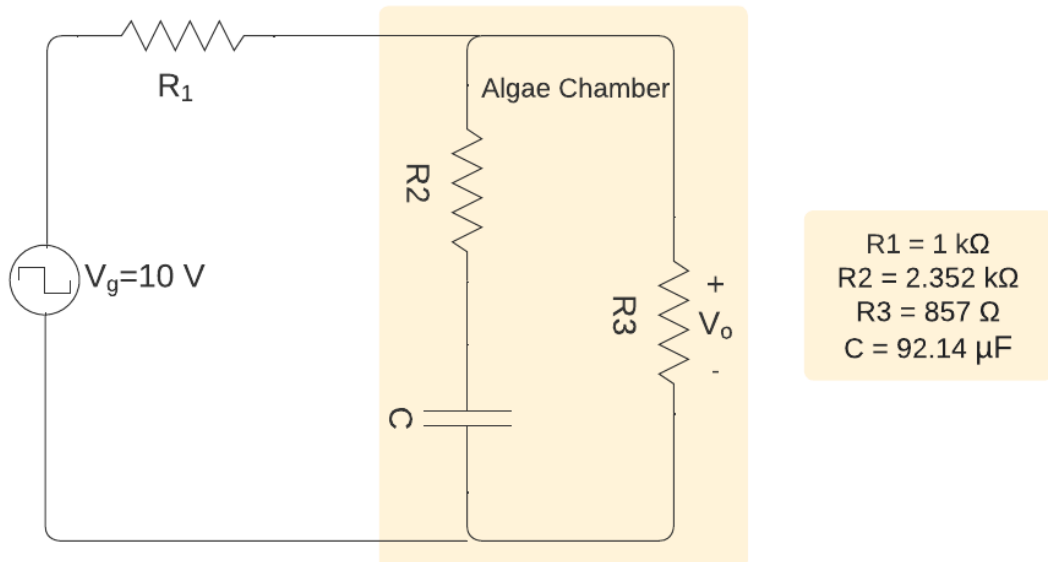
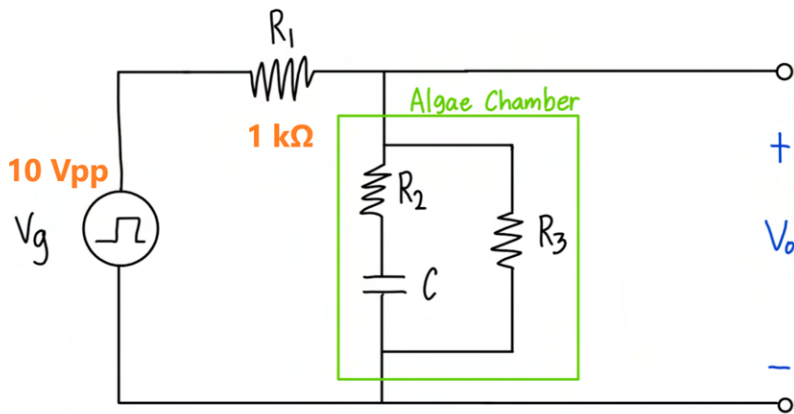


Fig. 3-6. Final Algae Chamber Model for  $V_g = 10\text{V}$

### 3.3 Algae Chamber I-V Model vs. Algae Species

The original model was developed using the *Desmodesmus Armatus* species. *Chlorella sp.* and *S. Obliquus* are used in present experiments. Two algae chamber models were created for the new strains, demonstrated by Fig 3-7.



| <u>Chlorella sp. Algae</u><br><u>Species</u> | <u>S. Obliquus Algae</u><br><u>Species</u> |
|--|--|
| <b>R2 = 1316 Ω</b>                           | <b>R2 = 233 Ω</b>                          |
| <b>R3 = 1189 Ω</b>                           | <b>R3 = 174 Ω</b>                          |
| <b>C = 8.857 uF</b>                          | <b>C = 55.561 uF</b>                       |

Fig. 3-7. Algae Chamber Model  $R_2$ ,  $R_3$ , and  $C$  - Chlorella sp., S. Obliquus Algae  
(Note: *Desmodesmus Armatus* original chamber model measurements  $R_2 = 2,352 \Omega$ ,  $R_3 = 857 \Omega$ ,  $C = 92.14 \mu F$ )

Figs. 3-8 and. 3-9 shows the relationship between chamber resistance and voltage in response to a 0-10 V, 3-second ramp input wave. Each plot calculates  $R_3$  for that species.  $R_3$  represents the algae steady-state resistance.

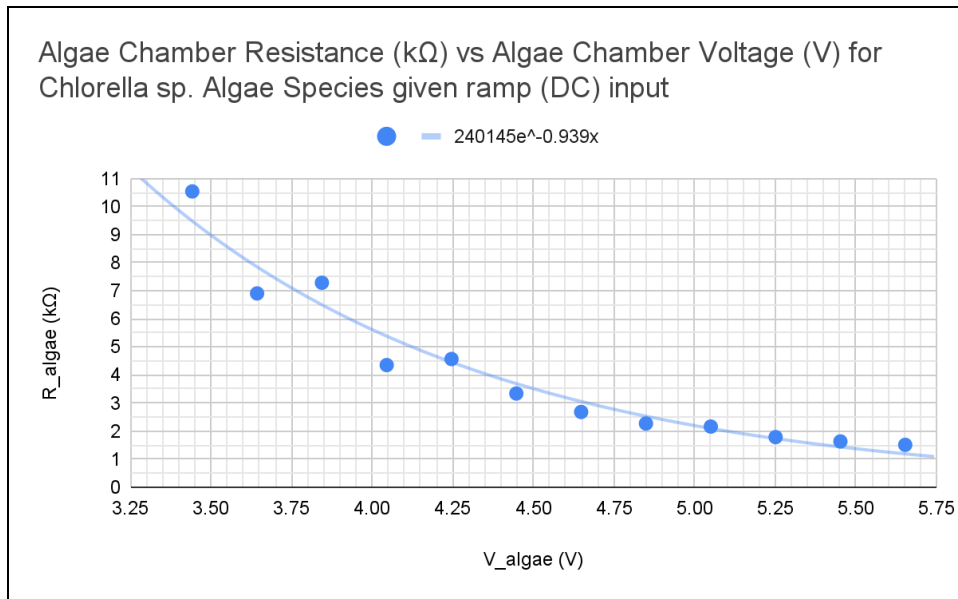


Fig. 3-8. Chamber resistance vs voltage output 10 Vpp, 5 VDC, 500 mHz Ramp Input.

*Chlorella sp.* grown in 83% growth medium, 17% water.

(Note: This represents the steady state characteristics of the chamber, where R<sub>algae</sub> corresponds to R<sub>3</sub> in Fig. 3-7)

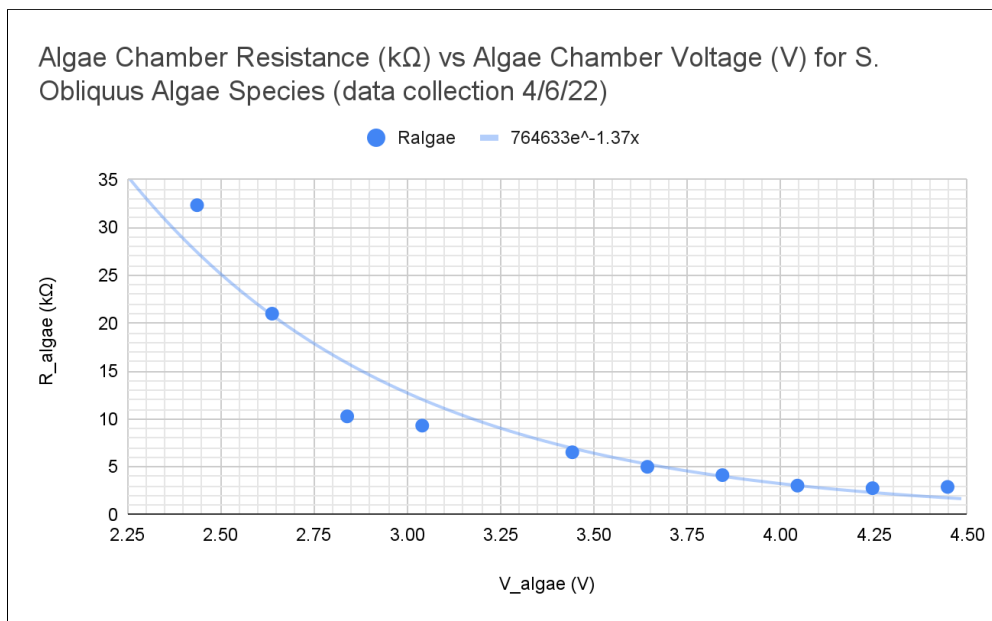


Fig. 3-9. Chamber resistance vs voltage output 10 Vpp, 5 VDC, 333.3 mHz Ramp Input.

*S. Obliquus* grown in 100% growth medium

Fig. 3-10 and Fig. 3-11 represent step responses of:

- i) *Chlorella* sp. algae 10 Vpp, 5 V<sub>DC</sub>, 500 mHz input square wave and
- ii) *S. Obliquus* algae 10 Vpp, 5 V<sub>DC</sub> 333.3 mHz input square wave.

Figures 3-10 and 3-11 define the required voltages and times to determine V<sub>o</sub>, τ, R<sub>2</sub>, and C using the following equations.

$$\text{Algae impedance} = R_3$$

$$V_o(t) = A + Be^{-t/\tau} = V_o(\infty) + [V_o(0) - V_o(\infty)] \quad (3-12)$$

$$V_o(0) = A + B \quad (3-13)$$

$$V_o(\infty) = A \quad (3-14)$$

$$R_2 = \frac{1}{\frac{V_g}{V_o(0)R_1} - \left(\frac{1}{R_3} + \frac{1}{R_1}\right)} \quad (3-15)$$

$$\begin{aligned} R_{eq} &= R_1 + R_2 \parallel R_3 \\ C &= \frac{\tau}{R_{EQ}} \end{aligned} \quad (3-16)$$

Table 3-3 shows *Chlorella sp.* model parameters. Table 3-4 shows *S. Obliquus* model parameters.

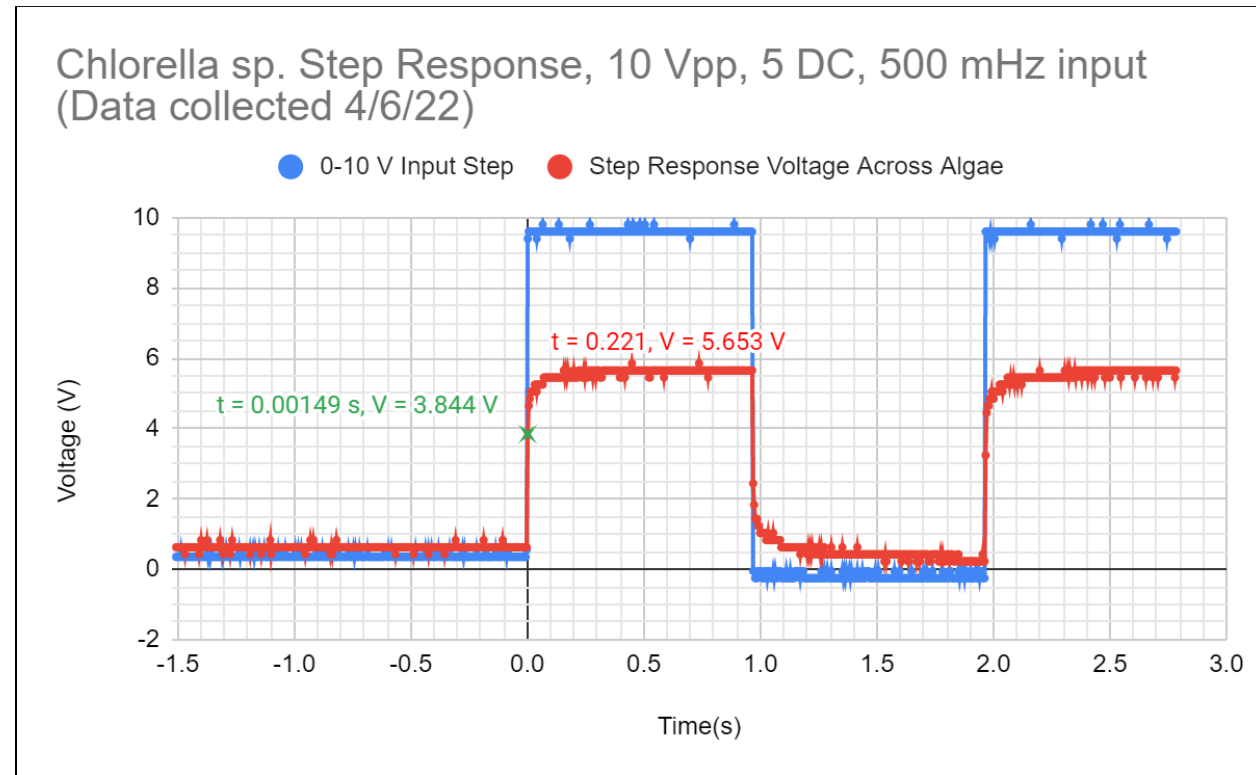


Fig. 3-10: *Chlorella sp.* Step Response 10 Vpp, 5 VDC, 500 mHz Square Input. Grown in 83% medium, 17% water.

**TABLE 3-3**  
Chlorella sp. Chamber Model Summary

| Parameter   | Value | Units         |
|-------------|-------|---------------|
| $V_g$       | 10.00 | V             |
| $V(\infty)$ | 5.653 | V             |
| $V(0)$      | 3.844 | V             |
| $t_{rise}$  | 0.221 | s             |
| $V(\tau)$   | 4.984 | V             |
| $\tau$      | 0.014 | s             |
| $R_1$       | 1000  | $\Omega$      |
| $R_3$       | 1189  | $\Omega$      |
| $R_2$       | 1316  | $\Omega$      |
| C           | 8.857 | $\mu\text{F}$ |

S. Obliquus Step Response, 10 Vpp, 5 VDC, 333.3 mHz input  
 (Data collected 4/6/22)

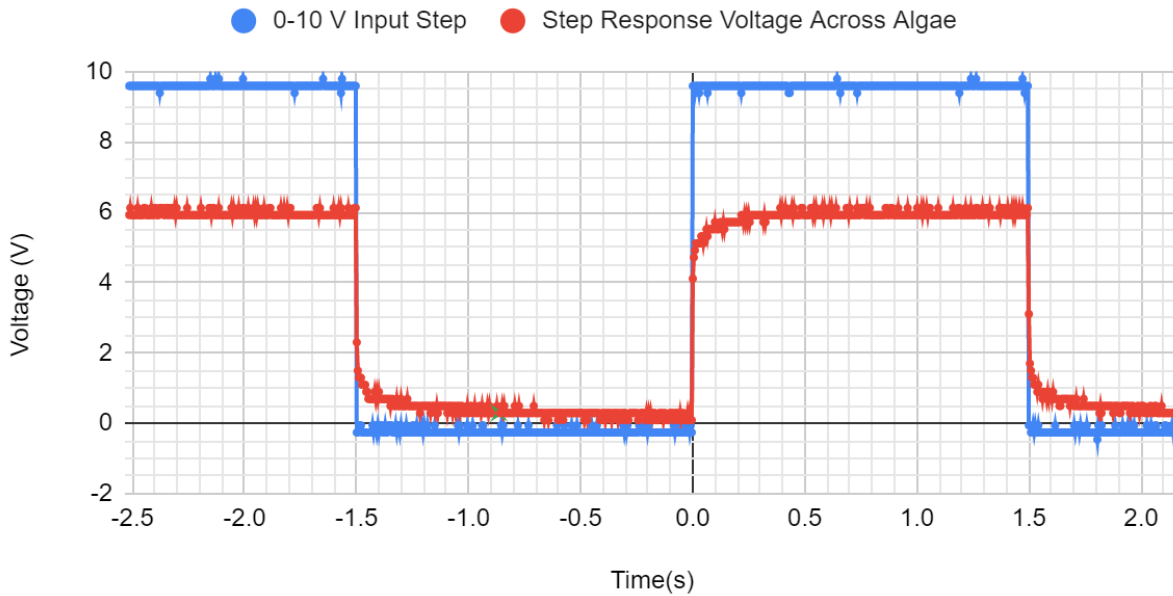


Fig. 3-11 *S. Obliquus* Step Response 10 Vpp, 5 VDC, 333.3 mHz Ramp Input. Grown in 100% growth medium

*TABLE 3-4*  
 S. Obliquus Chamber Model Values Summary

| Name        | Value  | Units    |
|-------------|--------|----------|
| $V_g$       | 10.00  | V        |
| $V(\infty)$ | 6.121  | V        |
| $V(0)$      | 4.111  | V        |
| $t_{rise}$  | 0.400  | s        |
| $V(\tau)$   | 5.377  | V        |
| $\tau$      | 0.061  | s        |
| $R_1$       | 1000   | $\Omega$ |
| $R_3$       | 174    | $\Omega$ |
| $R_2$       | 233    | $\Omega$ |
| C           | 55.561 | $\mu F$  |

### 3.3.1 ITO Glass Slides

When exposing the Algae Chamber to DC Voltage (e.g. 10Vdc, for more than 5 seconds), the ITO slide coating begins to “burn” as the Indium Tin Oxide decomposes. This is caused by intermittent current between the two ITO glass slides. Burnt ITO coating changes from transparent to opaque and becomes rough to the touch. Tiny gas bubbles (containing O<sub>2</sub>, CO, CO<sub>2</sub>, and N<sub>2</sub>) begin to form within the plates during decomposition. Burnt ITO glass slides decrease conductivity, yielding inconsistent pulse results. Fig. 3-12 shows fresh ITO glass slides (top) compared to burnt ITO glass slides (bottom).

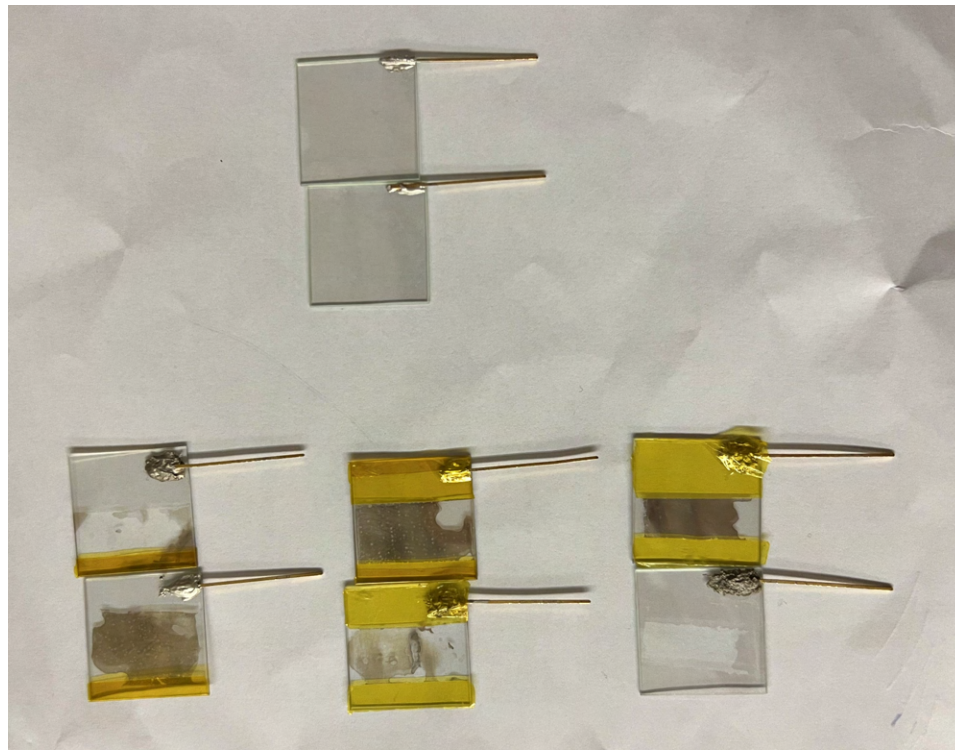


Fig. 3-12. Original (top) vs. Damaged (Bottom) ITO glass slides

**Solution:** Exercise caution when exposing any DC voltage to the Algae chamber. To generate a single pulse with the function generator, use the Pulse function, set frequency to 200mHz (5 seconds period), and set the duty cycle to 0.01 % to limit pulse width to only 500μs. Turn off function generator output after the pulse is applied.

### 3.4 Results

To calculate required PEF parameters, the Low-side electroporator circuit is used to treat algae samples. We load the ITO chamber with a  $15\mu\text{L}$  algae solution. The circuit connects to the ITO chamber using alligator clips. The Arduino program (Appendix A) controls the Pulse Length and Number of Pulses while the function generator controls Voltage (directly correlated to Field Intensity:  $E = \frac{V_{Chamber}}{30\ \mu\text{m}}$ .

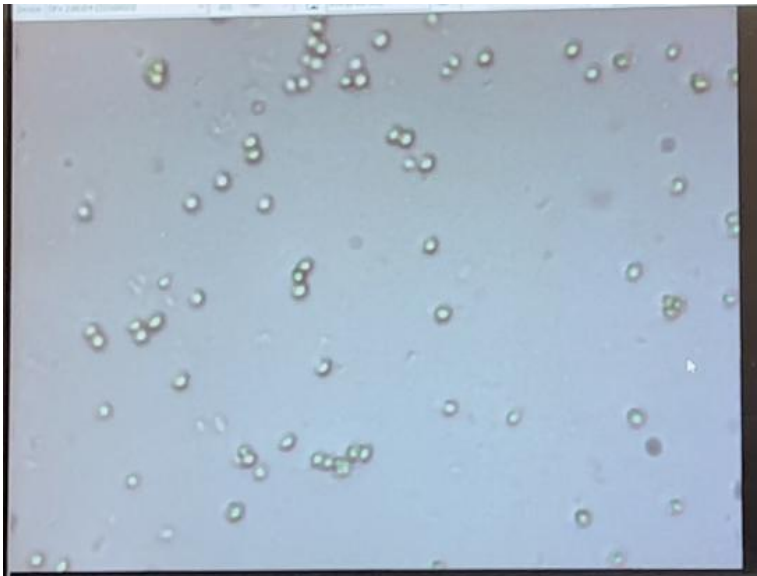
To determine algae lyses, we use a visual microscope to observe changes. Lysis indications include cell distortion, rapid movement, cell fragment, and scattered cell contents. Fig.3-13 shows a slide before and after pulses. No observable change occurred. Table. 3-5 summarizes lysing attempts using variable voltages and pulse parameters.

TABLE 3-5  
ALGAE TREATMENT TRIALS

| Case | Voltage | Field Intensity [MV/m] | Arduino Pulse Length | # Pulses | Visible Change (Chlorella) | Visible Change (Obliquus) |
|------|---------|------------------------|----------------------|----------|----------------------------|---------------------------|
| 1    | 100 V   | 3.33                   | 15 $\mu\text{s}$     | 10       | No                         | No                        |
| 2    | 150 V   | 5.0                    | 15 $\mu\text{s}$     | 10       | No                         | N/a <sup>2</sup>          |
| 3    | 200 V   | 6.66                   | 15 $\mu\text{s}$     | 10       | No                         | No                        |
| 4    | 250 V   | 8.33                   | 15 $\mu\text{s}$     | 10       | No                         | No                        |
| 5    | 300 V   | 10.0                   | 15 $\mu\text{s}$     | 20       | No                         | No                        |
| 6    | 300 V   | 10.0                   | 15 $\mu\text{s}$     | 30       | No                         | N/a                       |
| 7    | 300 V   | 10.0                   | 50 $\mu\text{s}$     | 10       | No                         | N/a                       |
| 8    | 300 V   | 10.0                   | 50 $\mu\text{s}$     | 30       | No                         | No                        |

<sup>2</sup> Some variables were not tested due to time constraints and circuit damage

Algae Samples after 10 15- $\mu$ s pulses at 250V (Case 4), x200 Magnification



Before Pulses



After Pulses

Fig. 3-13. Chlorella sp. Microscope Images, Before and After 10 250 V, 15 us Pulses

*TABLE 3-6*  
ALGAE TREATMENT TRIALS IN DEIONIZED WATER

| Case | Voltage | Field Intensity [MV/m] | Arduino Pulse Length | # Pulses | Visible Change (Obliquus) |
|------|---------|------------------------|----------------------|----------|---------------------------|
| D-1  | 100 V   | 3.33                   | 15 $\mu$ s           | 10       | No                        |
| D-2  | 300 V   | 10.0                   | 50 $\mu$ s           | 100      | No                        |

### 3.5 Discussion

None of the attempts resulted in algae lysis, despite voltages and durations exceeding the published results which utilized five 3 $\mu$ s pulses at 20-25kV/cm [11] and twenty-one 100 $\mu$ s pulses at 2.7 kV/cm [12]. Two hypotheses explain this failure. First, the algae medium contains ions, which could form charged layers on the ITO plates. The electric field exists in these layers and not across the algae. Table 3-6 shows two attempts using deionized water to wash the algae sample to test this hypothesis but it is not exhaustive. The second hypothesis is that something prevents E-field application across algae samples with the ITO chamber design or construction. The leads, epoxy, and plate conductivity could be inadequate to apply fields across the media. Alternatively, if Kapton tape is folded or the chamber is partially filled, the separation could be much larger than 30 $\mu$ m. Larger separation decreases field intensity, which potentially can lead to E-field below lysis requirements. A microscope or spectrometer could identify issues.

## **Chapter 4: Algae Classification Using Convolutional Neural Network**

### **4.1 Introduction**

#### **4.1.1 Goal**

Given pre- and post-treatment algae sample images/videos, use Machine Learning techniques to classify algae cells in an image.

#### **4.1.2 Background and Methods**

Deploying Neural Networks (NN) to perform object classification is popular in industry. As shown in Fig. 4-1, a trained Neural Network can process algae images, and identify algae species and provide location information. This information will quantify PEF treatment efficacy so we can compare treatments with automatic analysis. However, building and training a robust, efficient object classification NN can be difficult. Fortunately, many Machine Learning resources are available online open-source.

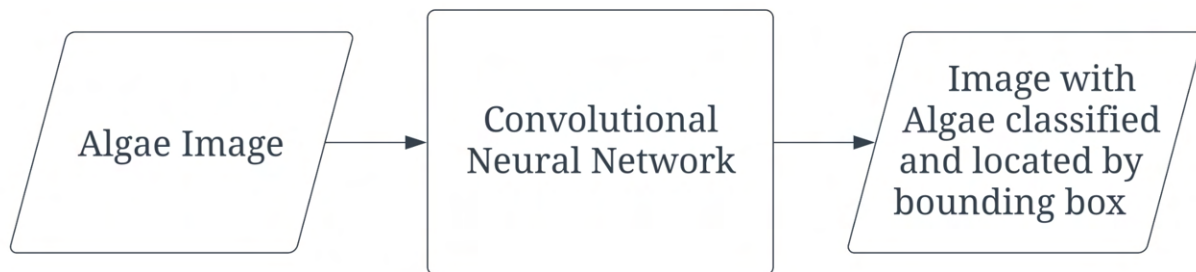


Fig 4-1. Flowchart of Neural Network performing Algae Classification

YOLOv5 is a popular object detection and classification algorithm [13] using Convolution Neural Network (CNN) architecture, under the Pytorch framework of Python. YOLOv5 provides a pre-trained model<sup>3</sup> containing weights adjusted during training to reduce the final classification error; then back-propagation is used to further update the weights, further reducing classification error.

We first trained with an open-source dataset, “coco128,” to understand the YOLOv5 pipeline. Using the same pipeline, several models were trained with our custom algae dataset, which includes 100 images of *Chlorella sp.* and 100 images of *S. Obliquus*.

This chapter discusses algae dataset creation and YOLOv5 model training. We assessed our trained model’s performance, its limitations and potential improvements. Finally, we evaluated the model’s potential in lysis analysis. For necessary Neural Network background and terminology information, refer to Appendix E.

<sup>3</sup> A *model* is a product of training a CNN, and is defined by its weight file, a set of parameters that defines the strength of connections between its many neurons.

## 4.2 Algae Species Information

### 4.2.1 Algae Strains

Our project works with two Algae strains: *S. Obliquus*, and *Chlorella sp.*, briefly described below. Culture Collection of Algae at UT-Austin assigns each strain of algae a unique UTEX number.

#### 1. UTEX 393- *Scenedesmus Obliquus*

- Oblong, some differences in morphology

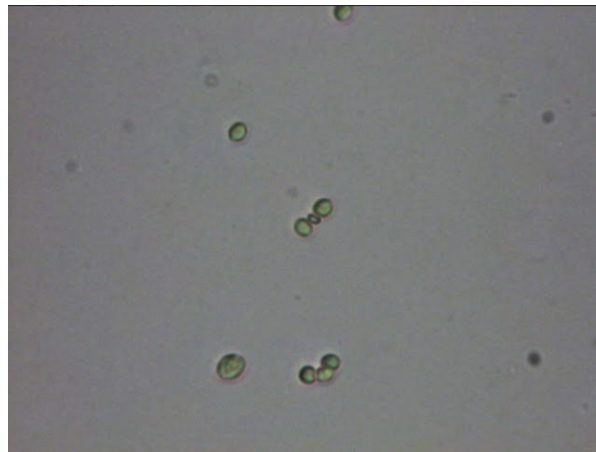


Fig 4-2. *S. Obliquus* Algae, 20x Lens

#### 2. UTEX 2714 - *Chlorella sp.*

- Circular, *Chlorella Vulgaris*

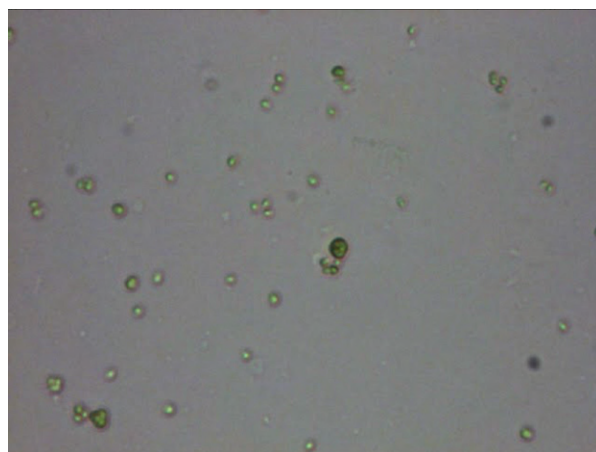


Fig 4-3. *Chlorella* Algae, 20x Lens

*TABLE 4-1.*  
ALGAE STRAINS CHARACTERISTICS

| Name                 | Mfr. Num. | Typical Size         | Notes  |
|----------------------|-----------|----------------------|--|
| <i>S. Obliquus</i>   | UTEX 393  | 8 - 13 $\mu\text{m}$ | <i>Tends to be round, oblong, and irregular.</i> |
| <i>Chlorella sp.</i> | UTEX 1412 | 2 - 10 $\mu\text{m}$ | <i>Tends to be circular</i>                      |

#### 4.2.2 Algae Image Data

*Acquisition Setting:* Windows Driver Model (WDM) Camera mounted on an Olympus Microscope Model CX43, connected to a desktop computer. *I.C. Capture 2.4* software [14] captures images and videos.

*Data Characteristics:*

- 640-by-480 pixel .bmp (Windows Bitmap File) images with 24-bit RGB.
- 640-by-480 pixel .avi (Audio Video Interleave) videos at 60 frames-per-second.

## 4.3 Convolutional Neural Network Approach

### 4.3.1 YOLOv5 Object Detection Algorithm

Convolutional Neural Network (CNN) is a supervised, deep learning algorithm that offers improved object classification, detection and image segmentation over traditional Artificial Neural Network (ANN) feed-forward design. A CNN implicitly combines ANN benefits while drastically increasing image classification efficiency by using convolution operations for feature extraction, which is manually-selected in ANN.

A popular real-time object detection algorithm used in industry is the You Only Look Once (YOLO) algorithm, first introduced in 2015 [14]. The original YOLO algorithm includes 24 convolutional layers followed by 2 fully connected layers. The output of this architecture is a  $7 \times 7 \times 30$  Tensor (matrix) of predictions, which is passed to a soft-max layer for classification. YOLO divides images into a grid system, and each grid cell is responsible for detecting objects within itself.

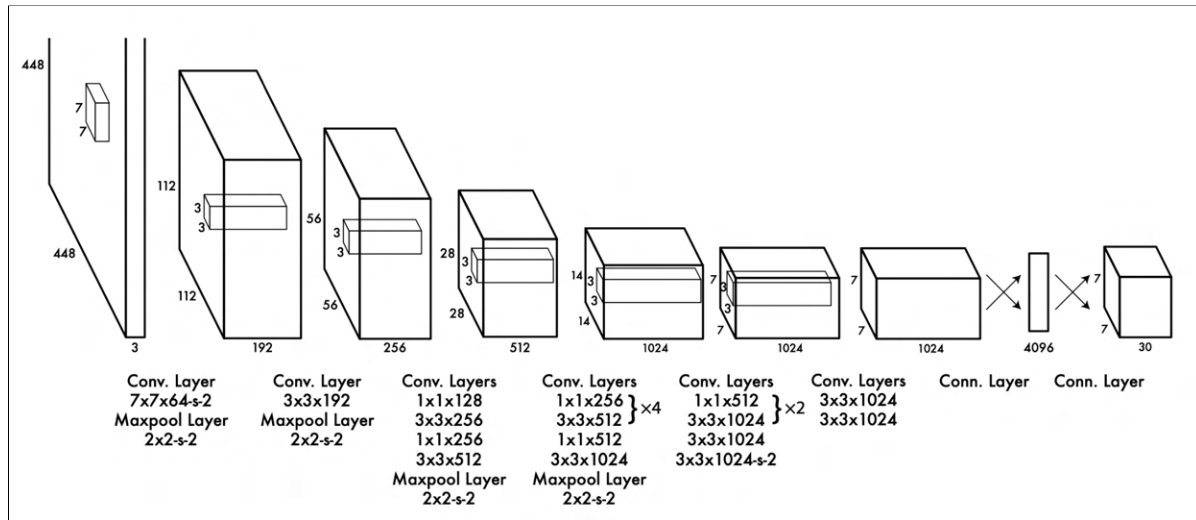


Fig. 4-4. YOLO Detection Network Architecture [14]

The latest YOLO version 5, YOLOv5 [15], is an optimized Python tensor library primarily used for Deep Learning applications using GPUs and CPUs. YOLOv5 is open source on Github. Compared to the original YOLO, YOLOv5 has improved the following [16]:

- Auto learning of anchor boxes (automatic addition)
- Use of cross-stage partial connections (CSP)
- Use of path aggregation (PAN) network
- Easier framework to train and test (PyTorch)
- YAML<sup>4</sup> file support - enhances the layout and model configuration file readability.
- Better data augmentation and loss calculations (Model is in PyTorch instead of C)

<sup>4</sup> YAML is a data serialization language that is used for writing configuration files.

### 4.3.2 Creating a Dataset of Algae Labels

#### Algae Image Capture

Supervised Learning using CNN architecture requires labeled datasets designed to train or “supervise” the CNN algorithm into classifying data or predicting outcomes. Using labeled inputs and outputs, the model measures its accuracy and learns over time.

YOLOv5 recommended custom dataset requirements:

- Images per class  $\geq$  1500 Images class
- Instances per class  $\geq$  10,000 (labeled objects) per class

Due to time constraints, only 100 images of *Chlorella sp.* and 100 images of *S. Obliquus* were captured. Fig. 4-6 below shows the dropbox folder containing *Chlorella sp.* images. All images were captured with *I.C. Capture 2.4 Software* in .bmp format. For each algae strain, every 25 images were recorded on fresh samples to guarantee image variety. The maximum magnification to retain resolution is 20x; the Algae Chamber does not accommodate a 40x lens.

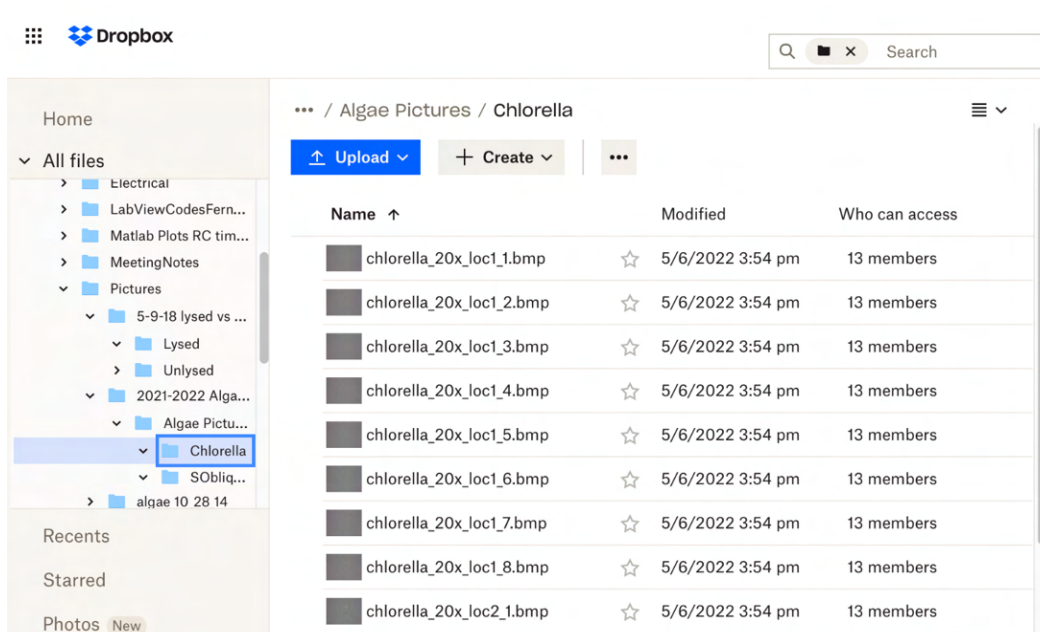


Fig 4-6. Dropbox Folder Containing 20x Lens *Chlorella sp.* Images

## Algae Image Labeling

To create labels for Algae Images, a Python GUI is used [18], as shown in Fig. 4-7. For each image, a bounding box (defined by 4 green dots on 4 corners) is drawn around each algae cell and assigned a “label” corresponding to the algae species.

Each algae image has a text file containing label and bounding box information, see Fig. 4-8 below. Each line contains an integer defining the class and two coordinate pairs that define the bounding box.

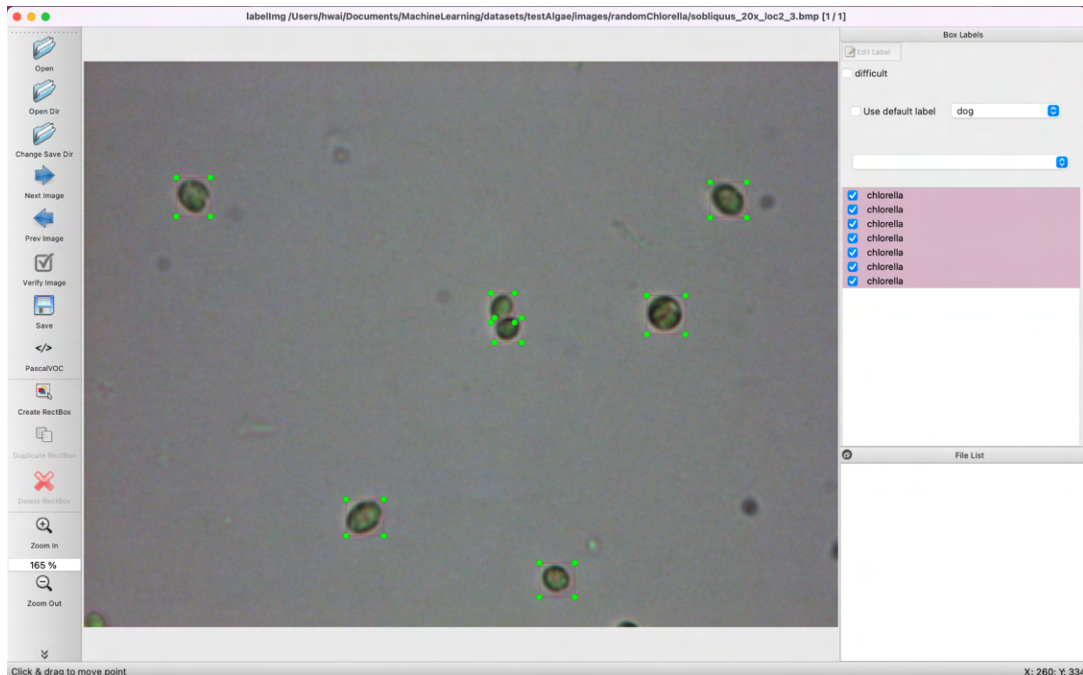


Fig. 4-7. Labeling Software GUI

```
datasets > coco128 > labels > train2017 > 000000000138.txt
1  72 0.122172 0.393944 0.192281 0.429529
2  74 0.546672 0.093979 0.107031 0.119546
3  45 0.281648 0.338351 0.071234 0.034084
4  69 0.499961 0.617976 0.187109 0.624712
5  71 0.877086 0.401291 0.201766 0.093403
6  58 0.910391 0.130305 0.06875 0.1026
7  75 0.3675 0.13712 0.052562 0.082304
```

Fig. 4-8. Example Image label.txt Information

### 4.3.3 YOLOv5 Algorithm with coco128 Dataset

#### coco128 Dataset

*coco128* is a dataset composed of the first 128 images in COCOtrain2017, Common Object in COntext [17] used for both training and validation to verify overfitting (classification capability). Fig. 4-9 is a representative image from *coco128*.



Fig. 4-9. Representative image from coco128 dataset

To reduce run time, one of the hyperparameters, “epoch,” is modified from the recommended 300 to 5, as shown in Fig. 4-10 below. “Epoch” is the number of repetitions the YOLOv5 algorithm executes through the entire dataset. Each Epoch requires approximately one minute of run-time, depending on hardware performance. Learning rate is maintained at 1%. ‘*yolov5s.pt*’ weight file contains the smallest and fastest pretrained weights to execute YOLOv5 on our dataset.

```
458     parser.add_argument('--data', type=str, default=ROOT / 'data/coco1
459     parser.add_argument('--hyp', type=str, default=ROOT / 'data/hyps/h
460     parser.add_argument('--epochs', type=int, default=5)
```

Fig. 4-10. Modified epoch hyperparameter from 300 to 5

The coco128 training set is executed with the following command [18], Fig. 4-11.

```
hwai@Hanks-MBP yolov5 % # Train YOLOv5s on COCO128 for 5 epochs
$ python train.py --img 640 --batch 16 --epochs 5 --data coco128.yaml --weights yolov5s.pt
```

Fig. 4-11. Running five coco128.yaml epochs

#### *Evaluation of YOLOv5 algorithm with coco128 dataset*

YOLOv5 algorithm output on the coco128 training set is shown in Fig. 4-14 below.

Overall, with only five epochs, precision is 79.4% and recall is 65.7%, and the calculated F-score is 0.719 or 71.9%. Since the weight file is pre-trained with a larger set of a COCO database, only minimal training on coco128 (a subset of the larger COCO database) is required to achieve such results.

```
Validating runs/train/exp10/weights/best.pt...
Fusing layers...
Model summary: 213 layers, 7225885 parameters, 0 gradients, 16.5 GFLOPs
      Class    Images    Labels      P      R   mAP@.5  mAP@.5:.95:
        all      128     929  0.794  0.657  0.764  0.504
```

Fig. 4-14. YOLOv5 Output Metric from five coco128.yaml Training Set epochs

#### 4.3.4 YOLOv5 Algorithm with custom Algae Dataset

Using the same coco128 pipeline and YOLOv5 algorithm, our custom Algae dataset containing 200 images is named as *randomAlgae*. An Algae image collage with labels is shown in Fig. 4-15 below.

- Label 15: *Chlorella sp.* algae species
- Label 16: *S. Obliquus* algae species

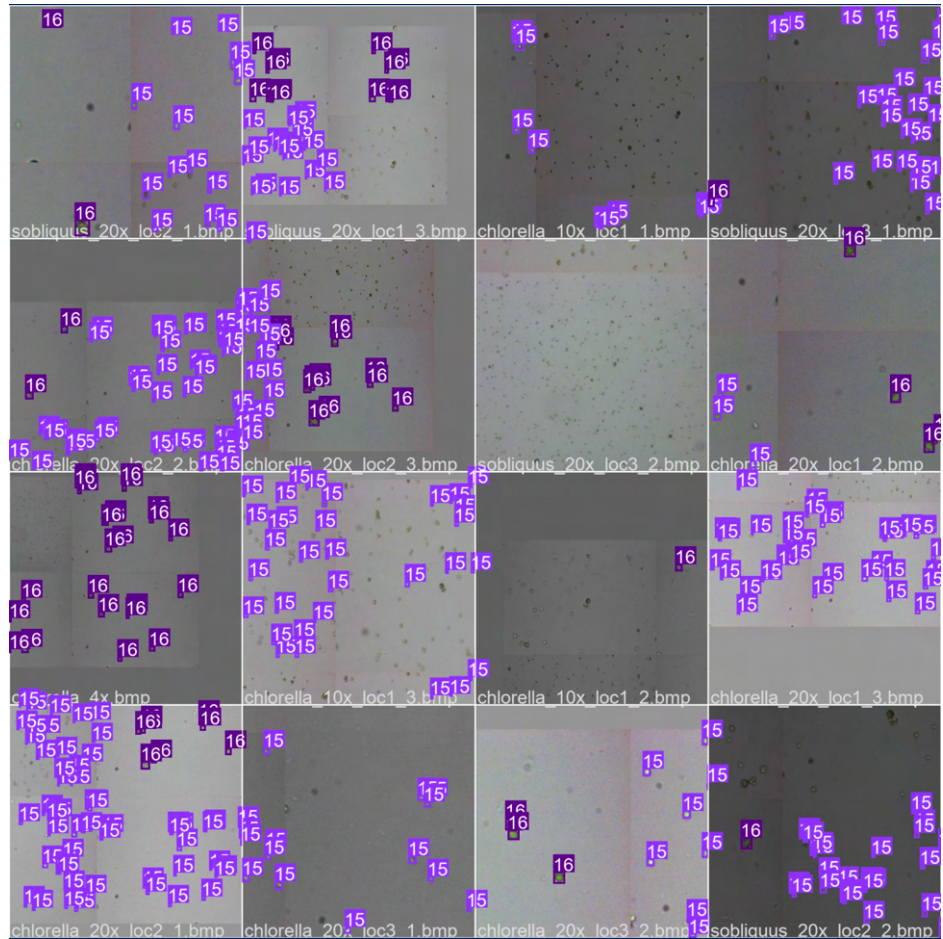


Fig. 4-15. “randomAlgae” Dataset Training Batch Collage

YOLOv5 algorithm outputs on the custom *randomAlgae* training set are shown in Figs. 4-16, 4-17, and 4-18 below. With 100 epochs (iterations), overall algae classification precision is 23.3%. *Chlorella sp.* classification Precision is 15.2%, and *S. Obliquus* is 31.4 %. As expected, Precision increases as the count of epochs increases: 0.0376% with 5 epochs, 1.35% with 10 epochs, 23.3% with 100 epochs, Recall also increases from 0.725% with 5 epochs, 2.9% with 10 epochs, 45.1% with 100 epochs. Higher metric scores are expected with more epochs, but these models may be inaccurate, as discussed in 4.3.5.

| Model summary: 213 layers, 7055974 parameters, 0 gradients, 15.9 GFLOPs |        |        |          |         |          |             |
|---|--------|--------|----------|---------|----------|-------------|
| Class   | Images | Labels | P        | R       | mAP@.5   | mAP@.5:.95: |
| all   | 200    | 3230   | 0.000376 | 0.00725 | 0.000164 | 3.29e-05    |

Fig. 4-16. YOLOv5 Output Metric from 5 Epochs of Algae Training Set

| Model summary: 213 layers, 7055974 parameters, 0 gradients, 15.9 GFLOPs |        |        |        |       |         |             |
|---|--------|--------|--------|-------|---------|-------------|
| Class   | Images | Labels | P      | R     | mAP@.5  | mAP@.5:.95: |
| all   | 200    | 3230   | 0.0135 | 0.029 | 0.00312 | 0.000312    |

Fig. 4-17. YOLOv5 Output Metric from 10 Epochs of Algae Training Set

| Model summary: 213 layers, 7055974 parameters, 0 gradients, 15.9 GFLOPs |        |        |       |       |        |             |
|---|--------|--------|-------|-------|--------|-------------|
| Class   | Images | Labels | P     | R     | mAP@.5 | mAP@.5:.95: |
| all   | 200    | 3230   | 0.233 | 0.451 | 0.222  | 0.0583      |
| chlorella   | 200    | 2542   | 0.152 | 0.512 | 0.187  | 0.0405      |
| sobliquus   | 200    | 688    | 0.314 | 0.391 | 0.256  | 0.0762      |

Fig. 4-18. YOLOv5 Output Metric from 100 Epochs of Algae Training Set

#### 4.3.5 Convolution Neural Network (CNN) Performance Evaluation

Although additional YOLOv5 algorithm epochs on the Algae Dataset improves the Precision Metric and classification accuracy, the trained YOLOv5 model is inaccurate due to the following reasons:

1. *Overtraining*: There is a high probability of overtraining: when a neural network model predicts training samples with high accuracy (90% -100%), but fails to generalize to new data (low confidence score on detected objects). This leads to poor performance when the model is actually deployed in the field. Usually, overtraining is due to insufficient data or excessively homogeneous data.
2. *Insufficient Data*: Due to time constraints, only 100 images of each strain of Algae are captured and labeled, far from the recommended minimum of 1500 images **per** class. A total of 3230 Algae objects have been labeled, also significantly less than the recommended minimum of 10,000 labels **per** class.
3. *Invariant Images*: Algae images are captured under invariant lighting conditions with the same microscope. For “real-world” representative datasets, images must be acquired from different sources under variable lighting.
4. *Inaccurate Labels*: Each Bounding box should tightly enclose an Algae’s edge, leaving no space in between the box and the Algae’s edge, but there could be mislabeling due to laboratory negligence (poorly drawn bounding boxes when labeling) . In addition, there may be unlabeled Algae cells.
5. *Resolution and Algae Shape*: Limited camera resolution may blur algae cell edges, resulting in feature loss. *Chlorella sp.* (2 - 10 $\mu$ m) and *S. Obliquus* (8 - 13  $\mu$ m) are different sizes; the two algae strains closely resemble each other in shape and color. CNNs are not rotation nor scale invariant; thus, limited camera resolution and a mixture of algae Images captured with 10x lens and 20x lens (10x lens yields poor resolution for labels) may increase algae misclassifications.

In summary, Convolutional Neural Networks for Algae classification is promising, but the above concerns must be addressed to optimize results.

#### **4.3.6 Further Application**

YOLOv5 algorithm used to train models for Algae Classification can also be used in algae cell lysis analysis. In a new algae dataset, there could be images of pre-lysed and post-lysed algae. Areas of microalgal lipid content can be labeled as ‘lysed’.

## **Chapter 5: Conclusion**

In this report, we defined and outlined required parameters for a rectangular pulsed electric field to lyse algae. To aid our circuit design, we tested algae and developed an improved algae impedance model. We developed a low-side switching capacitive circuit capable of meeting and exceeding our requirements. However, in testing, this circuit failed to lyse algae in all trials. The reasons are currently unknown, but likely relate to the chemistry of the algae media or ITO chamber construction.

For future experiments, it is necessary to examine why the circuit fails, including testing with deionized water and improving ITO Chamber manufacturing techniques. Additionally, there are several ways to improve the electroporator circuit to increase efficiency or improve performance if necessary, discussed in the design section.

## Appendix A: Arduino Pulse Code

```
const int ssr1=8; // Charge Switch
const int ssr2=9; // Relay Switch
const int fet1=10; // Pulse Control
const int fet2=11; // Capacitor Discharge Switch
const int num_pulses = 100; // number of pulses
const bool discharge_immed = false; // Discharge and then wait without running
pulses
const bool discharge_post = true; // Discharge after running pulses

void setup() {
    //set up output pins
    pinMode(ssr1, OUTPUT);
    pinMode(ssr2, OUTPUT);
    pinMode(fet1, OUTPUT);
    pinMode(fet2, OUTPUT);
    //initiate no charge, chamber low
    digitalWrite(ssr1, LOW);
    digitalWrite(ssr2, LOW);
    digitalWrite(fet1, LOW);
    digitalWrite(fet2, LOW);
}
void loop() {
    if(discharge_immed){
        digitalWrite(fet2, HIGH);
        digitalWrite(ssr2,HIGH);
        while(1){
            // Keep the capacitor in a discharged state
        }
    }
}

// -- Charging Phase -- //
digitalWrite(ssr1, HIGH); //Begin Charging the Storage Capacitor
delay(60000);
digitalWrite(ssr1, LOW); //Disconnect the Storage Capacitor from the DC amplifier
digitalWrite(ssr2,HIGH); //Begin Discharging the Storage Capacitor
delay(5); // Wait for Discharge Switch to turn on

// -- Pulsing Phase -- //
int current_pulse = 0;
while(current_pulse < num_pulses){ //start sending pulses to the load
    digitalWrite(fet1, HIGH); // Chamber High Voltage
    delayMicroseconds(15);
    digitalWrite(fet1, LOW); // Chamber Low Voltage
    delayMicroseconds(15);
    current_pulse++;
}
```

```
}

//digitalWrite(ssr2, LOW); // Testing chamber holding capacity
//delay(5);
if(discharge_post){
    digitalWrite(fet2, HIGH); // Discharge the capacitor
    //digitalWrite(fet1, HIGH); // Test chamber holding capacity
}
while(1){
    // Don't loop back to pulsing, just wait in post.
}
}
```

## Appendix B: Electroporator Bills of Materials and Timeline

*TABLE B-1.*  
LOW-SIDE SWITCHING COMPONENT COST ESTIMATE

| Part                  | Description            | Quantity | Unit Cost | Total Cost | Justification   |
|-----------------------|------------------------|----------|-----------|------------|---|
| ALA7DA56<br>1EE500    | Electrolytic Capacitor | 1        | \$14.74   | \$14.74    | Storage capacitor used to hold 0-300 V pulse voltage          |
| CPC1779J              | Solid-State Relay      | 2        | \$10.97   | \$21.96    | Act as current protection relay                               |
| TPH3208               | GaNFET                 | 2        | \$10.47   | \$20.94    | Acts as switches to control the pulse duration.               |
| -                     | Resistor (Various)     | 5        | -         | -          | Required for overcurrent protection                           |
| MUR420 A0G            | Diode                  | 1        | \$0.95    | \$0.95     | Guides current to flow in the intended direction              |
| CFR-12JR-5<br>2-1K    | Arduino Kit            | 1        | \$54      | \$54       | Use MCU to send clock signal to the relays                    |
| -                     | Gauge 20 Wire          | 0.5 m    | -         | -          | Connect electronic components together on the prototype board |
| -                     | ITO coated glass       | 2        | \$15      | \$30       | Needed to construct the electromagnetic field chamber         |
| Trek Model<br>601C    | DC Voltage Amplifier   | 1        | -         | -          | Amplifier signals to output high voltage supply               |
|                       | Function Generator     | 1        | -         | -          | Provide low voltage input to the DC voltage amplifier         |
| AM-Scope<br>40X-1000X | Microscope             | 1        | -         | -          | Observe the shape of the algae cells after the treatment      |
| <b>Subtotal</b>       |                        |          |           |            | \$142.6   |
| <b>Shipping</b>       |                        |          |           |            | \$4.99  |
| <b>Total</b>          |                        |          |           |            | \$147.59  |

*TABLE B-2.*  
INDUCTIVE ELECTROPORATOR COMPONENT COST ESTIMATE

| Circuit Components        | Part Number                                | Price   | Quantity   | Total          |
|---------------------------|--|---------|------------|----------------|
| R - 6Ω, 50W               | <a href="#"><u>PWR221T-50-6R00F-ND</u></a> | \$4.03  | 1          | \$4.03         |
| R - 50Ω, 50W              | <a href="#"><u>696-1352-ND</u></a>         | \$4.61  | 1          | \$4.61         |
| 100 Ω Potentiometer, 50 W | <a href="#"><u>AVT50-100-ND</u></a>        | \$7.56  | 1          | \$7.56         |
| L - 10uH, 5A              | <a href="#"><u>AIUR-06-100K-ND</u></a>     | \$1.08  | 1          | \$1.08         |
| L - 22uH, 5A              | <a href="#"><u>732-1418-ND</u></a>         | \$2.72  | 1          | \$2.72         |
| L - 33uH, 5A              | <a href="#"><u>553-1122-ND</u></a>         | \$4.83  | 1          | \$4.83         |
| L - 40uH, 5A              | <a href="#"><u>HM3335-ND</u></a>           | \$6.41  | 1          | \$6.41         |
| L - 50uH, 5A              | <a href="#"><u>553-1121-ND</u></a>         | \$4.59  | 1          | \$4.59         |
| Additional                |  |         |            |                |
| Rotary Switch             | <a href="#"><u>360-2379-ND</u></a>         | \$17.61 | 1          | \$17.61        |
| Heat Sinks                | <a href="#"><u>HS523-ND</u></a>            | \$0.95  | 2          | \$1.90         |
| Bind Post Black           | <a href="#"><u>J10126-ND</u></a>           | \$3.62  | 1          | \$3.62         |
| Bind Post Red             | <a href="#"><u>J10125-ND</u></a>           | \$3.62  | 1          | \$3.62         |
|                           |  |         | <b>SUM</b> | <b>\$62.58</b> |

*TABLE B-3*  
HIGH-SIDE SWITCHING COMPONENT COST ESTIMATE

| Circuit Component                                 | Price                        | Quantity | Total           |
|---|------------------------------|----------|-----------------|
| GaNFET (TPH3208)                                  | \$10.47                      | 3        | \$ 31.41        |
| SSR (CPC1779J)                                    | \$10.91                      | 2        | \$ 21.82        |
| Diode (1N4007)                                    | (From Arduino Kit)           | 3        | N/A             |
| Resistor (10kΩ)                                   | (From Arduino Kit)           | 3        | N/A             |
| Resistor (1kΩ)                                    | (From Arduino Kit)           | 1        | N/A             |
| Resistor (100 Ω)                                  | (From Arduino Kit)           | 2        | N/A             |
| Resistor (10 Ω)                                   | (From Arduino Kit)           | 1        | N/A             |
| Capacitor (100 nF)                                | (From Arduino Kit)           | 1        | N/A             |
| Capacitor<br>(MAL215943681E3)<br>(680 μF/ 250Vdc) | \$13.04<br>(Provided in lab) | 1        | \$13.04         |
| Arduino Uno                                       | \$23<br>(From Arduino Kit)   | 1        | \$23            |
| <b>Sum</b>  |                              |          | <b>\$ 89.26</b> |

TABLE B-4  
LABOR COST ESTIMATE

|          | # People | Expected Working Hour   | Wage          | Medicare (1.45%) | SSN (6.2%) | Total      |
|----------|----------|-------------------------|---------------|------------------|------------|------------|
| Advisors | 3        | 30 hr (1 hr/week)       | \$65/ hr [11] | \$0.9425/hr      | \$4.03/hr  | \$6297.525 |
| Students | 6        | 196.5 hrs (Gantt Chart) | \$32/ hr [12] | \$0.464/hr       | \$1.984/hr | \$40614.19 |
| Total    |          |                         |               | \$47,383.22      |            |            |

According to Career Explorer, the average entry level electrical engineering salary in California is \$31.78/hour going up to \$40.14/hour at the junior level. The annual salary of our professors is around \$100,000, so their hourly wage is probably around \$65. Based on the hours of labor shown in the following Gantt charts, the estimated working hour for each student is around 196.5 hours in this school year; the estimated working hour for each advisor is around 30 hours. After considering the added cost of Medicare and SSN, the total cost of labor adds up to \$47.383.22.

## Timeline

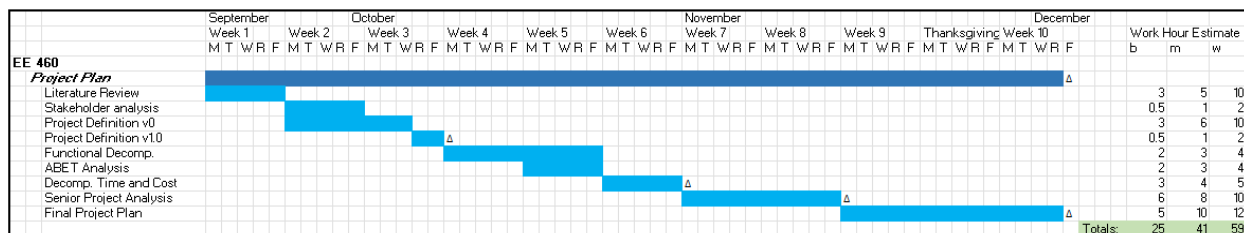


Fig. B-1: EE 460 Gantt Chart and Work Hour Estimates, including best, worst and most likely times.

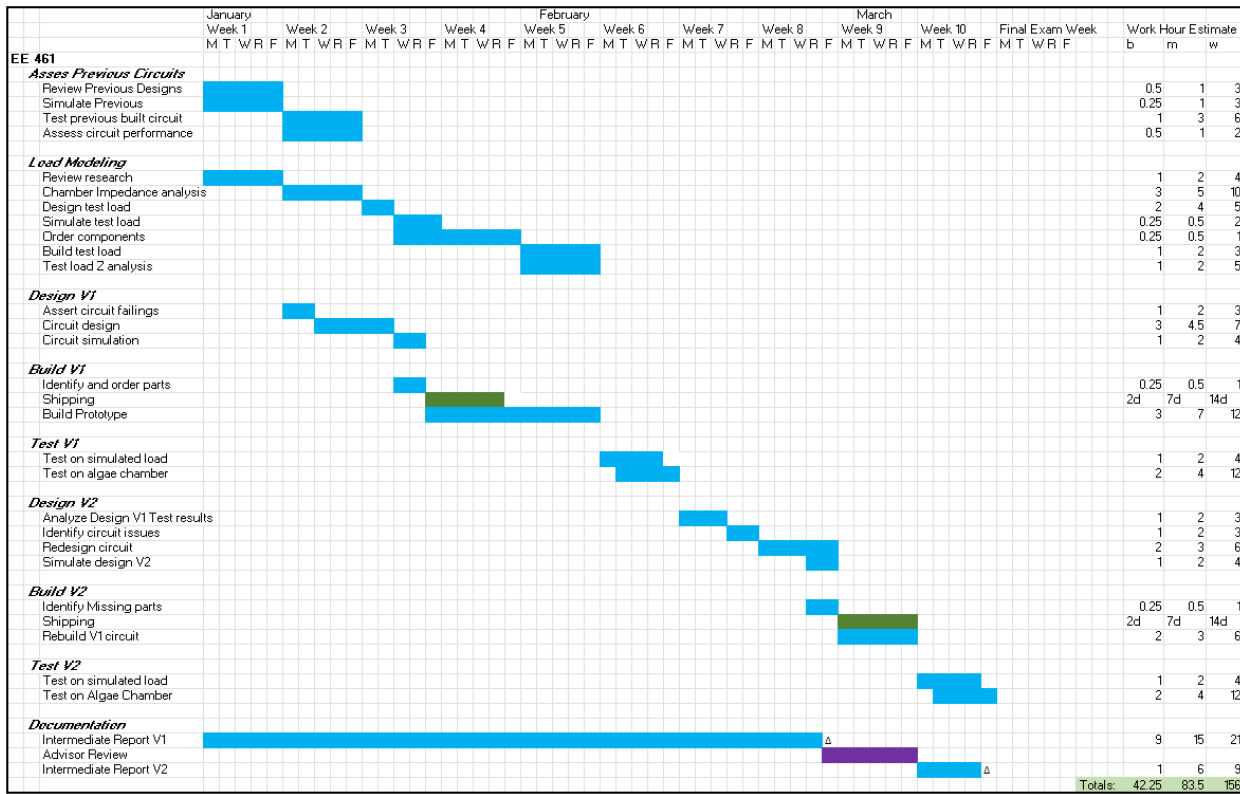


Fig. B-2: EE 461 Gantt Chart and Work Hour Estimates

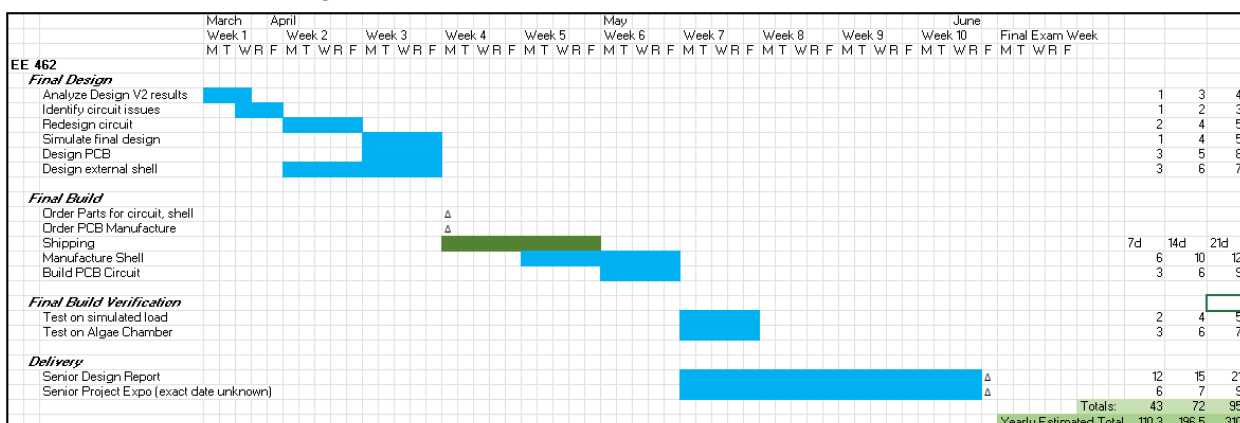


Fig. B-3: EE 462 Gantt Chart and Work Hour Estimates

## **Appendix C: Background & Terminology of Convolutional Neural Network**

**Features** are quantifiable data points used to analyze an object. For an algae cell, notable local features include radius, size, ellipticity, hue, etc.

A **label** defines object types in a dataset. For an algae cell, an object classification algorithm assigns labels such as *S. Obliquus*, *Chlorella*, *S. Capricornutum*, or *D. Armatus*, etc.

An **input image** is stored as a matrix of pixel values. Each pixel has a Red, Green, and Blue value. Each pixel contains three values, Red, Green, and Blue, referred to as channels. Each channel has a 2-dimensional matrix with integer values ranging from 0 to 255; each image has 3 channels stacking on top of each other. A typical algae image (Fig. 4-3) from our laboratory taken with the mounted camera on the Olympus Microscope is a 640 by 480 pixels TIFF file or BMP file, with 24-bit RGB values (8-bits for each channel).

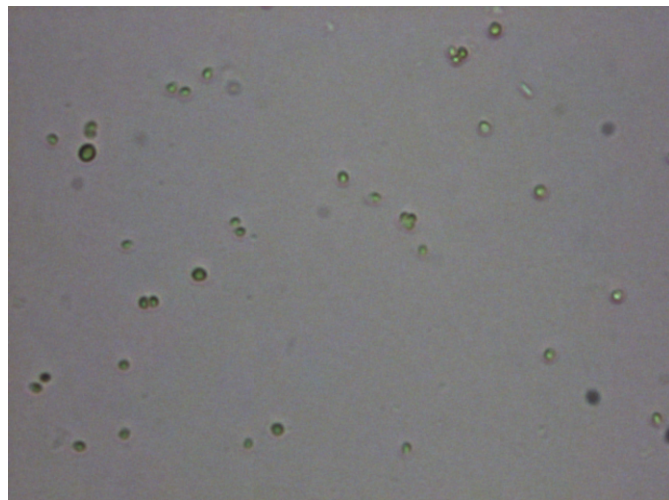


Fig E-1. *Chlorella* Algae, 20x Lens

A **kernel** filter extracts image features. The output is a matrix, the same size as the input, composed of the dot product of that image and the kernel matrix. For example, output pixel (1,1) is the dot product of input pixels (0,0) to (2,2) with a 3x3 kernel matrix. Sobel or Prewitt filters, Canny Edge Detectors, and Harris Corner Detectors Kernel filters detect features such as horizontal or vertical lines, edges, and corners. Fig. 4-4 below demonstrates edge detection using a Gaussian Filter.

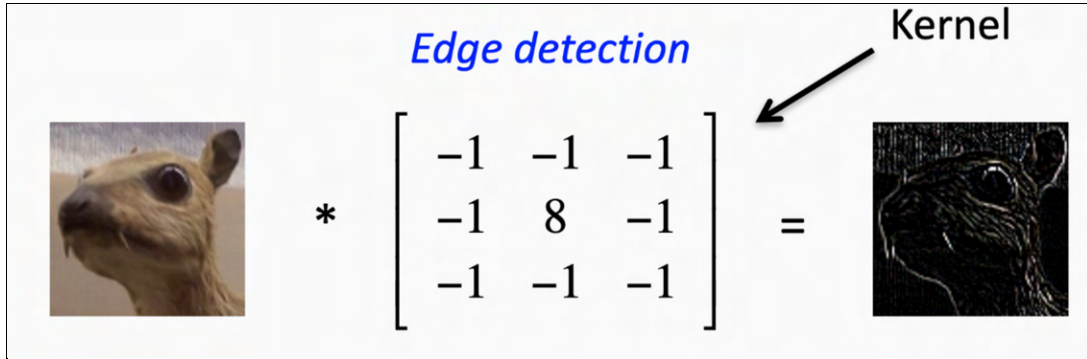


Fig. E-2. Edge Detection Kernel Demonstration

A **Convolution Layer** in a Convolutional Neural Network processes input images using one or several kernels and performs convolution operations to generate feature maps. Feature maps are matrices in the same dimension, but equal or smaller in sizes as input images. Pixels in close proximity generate a semantic meaning that contributes to an object's interpretation and identification. For example, a Convolution Layer can examine the green channel of an Algae image, then extract the tally of Green intensities within a neighborhood of pixels as a feature to store in one of its feature maps.

A **Pooling Layer** follows a Convolution Layer, and reduces feature map dimensionality to retain only the significant information. Pooling layers select the largest values on the feature maps and extend the results to subsequent layers. Generally, max pooling is used to retain the outliers, which strongly defines a certain feature.

A **Fully-Connected Layer** is in the final stages of a CNN. Fully connected layers flatten and compile data extracted from the previous layers to produce an output. This output is then passed through a series of *soft-max* layers. Soft-max layers use softmax activation functions to generate ‘confidence scores,’ or probabilities, of every label on the basis of the initial CNN input. For example, if an algae cell image yields a confidence score of 0.78 for *S. Obliquus* and 0.89 for *Chlorella sp.*, it will be classified as *Chlorella sp.*.

**IoU:** For detection, a common way to determine if an object classification is correct is *Intersection over Union* metric (*IoU*, *IU*) [19], a metric that allows us to evaluate how similar our predicted bounding box is to the ground truth bounding box. This combines the set *A* of proposed object pixels and the set of true object pixels *B* and calculates:

$$IoU(A, B) = \frac{A \cap B}{A \cup B}$$

Commonly, an IoU score  $> 0.5$  signifies success, otherwise failure. Fig. 4-12 below shows a sample of IoU scores with different bounding box configurations.

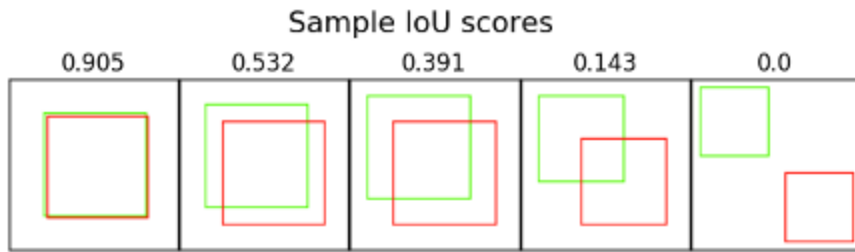


Fig. E-3. Sample of IoU scores

**Confusion Matrix** is a summary of prediction results on a classification problem. Shown in Figure X. is a confusion matrix of a binary classification for a positive class and a negative class, labeled  $P$  and  $N$ . Each row of the matrix corresponds to a predicted class, and each column of the matrix corresponds to an actual class.

|              |     | Predicted class      |                      |
|--------------|-----|----------------------|----------------------|
|              |     | $P$                  | $N$                  |
| Actual Class | $P$ | True Positives (TP)  | False Negatives (FN) |
|              | $N$ | False Positives (FP) | True Negatives (TN)  |

Fig. E-4. Binary Classification Confusion Matrix

**True Positive (TP)** is an outcome where the model correctly predicts the positive class.

i.e. when a *Chlorella sp.* algae cell is classified as *Chlorella sp.* algae cell

**False Positive (FP)** is an outcome where the model incorrectly predicts the positive class.

i.e. when an *S. Obliquus* algae cell is classified as *Chlorella sp.* algae cell

**True Negative (TN)** is an outcome where the model correctly predicts the negative class.

i.e. when a *S. Obliquus* algae cell is classified as *S. Obliquus* algae cell

**False Positive (FN)** is an outcome where the model incorrectly predicts the negative class.

i.e. when a *Chlorella sp.* algae cell is classified as *S. Obliquus* algae cell

**Precision** is calculated as the number of true positives divided by the total number of True Positives and False Positives, shown below. It is simply the ratio of correct positive predictions out of all

positive predictions made. Precision is a value between 0.0 for no precision, and 1.0 for full or perfect precision. Precision is useful, but fails to address how many false negatives there are. Maximizing precision will minimize the number of False Positives.

$$\text{Precision for class } c : \frac{TP(c)}{TP(c)+FP(c)} \quad (4-1)$$

i.e. Consider an algae dataset where the model predicts 150 cells belonging to the class *Chlorella sp.*, 95 of which are predicted correctly (true positives) and 55 of which are predicted incorrectly (false positives), the precision of classifying *Chlorella sp.* on this model is 63.3%.

**Recall** is a metric that quantifies the number of correct positive predictions made out of all positive predictions that could have been made, and serves as an indication of missed positive predictions. Recall is a value between 0.0 for no recall or 1.0 for full or perfect recall. Maximizing Recall will minimize the number of False Negatives.

$$\text{Recall for class } c : \frac{TP(c)}{TP(c)+FN(c)} \quad (4-2)$$

i.e. Consider an algae dataset where the model predicts 150 cells belonging to the class *Chlorella sp.*, 95 of which are predicted correctly (true positives) and 5 of which were missed (false negatives), the Recall of classifying *Chlorella sp.* on this model is 95%.

**F-score** provides a metric that combines properties of both Precision and Recall, since neither alone can tell the whole story. We can have excellent Precision and poor Recall, or poor Precision and excellent Recall. A perfect Precision and a perfect Recall will result in a perfect F-score of 1.0. The equation to calculate F-score is as follows:

$$\text{F-score} : \frac{2 * \text{Precision} * \text{Recall}}{\text{Precision} + \text{Recall}} \text{ or } \frac{1}{\frac{1}{\text{Precision}} + \frac{1}{\text{Recall}}} \quad (4-3)$$

i.e. Following the above Precision of 63.3% and Recall of 95%, the F-score is calculated to be 75.9%, which is a reasonable score. This is an example where good Recall levels-out poor Precision.

## Appendix D: Graphical User Interface (GUI) for Simplified Data Acquisition

### Agilent 33220A Arbitrary Waveform Generator GUI:



Fig. F-1. Agilent 33220A Arbitrary Waveform Hardware Front Panel

#### Description:

Utilizing LabVIEW 2021, this GUI allows the user to remotely control and automate the Agilent 33220A Arbitrary Waveform Generator via PC/Laptop and a simple USB connection. The project utilizes this waveform generator to produce the DC signal that powers the main pulsing circuit. [20]

#### Requirements:

- Agilent 33220A Arbitrary Waveform Generator
- USB A to USB B cable connection
- LabView 2021 Application
- GUI Project Files

#### Instructions:

1. First connect the PC/Laptop to the Waveform Generator using the USB connection cable.
2. Start LabView and open the WaveformGenerator.vi Project file.
3. After opening the Project file a simplified version of the Waveform Generators front panel should appear on screen. (Fig. F-2)

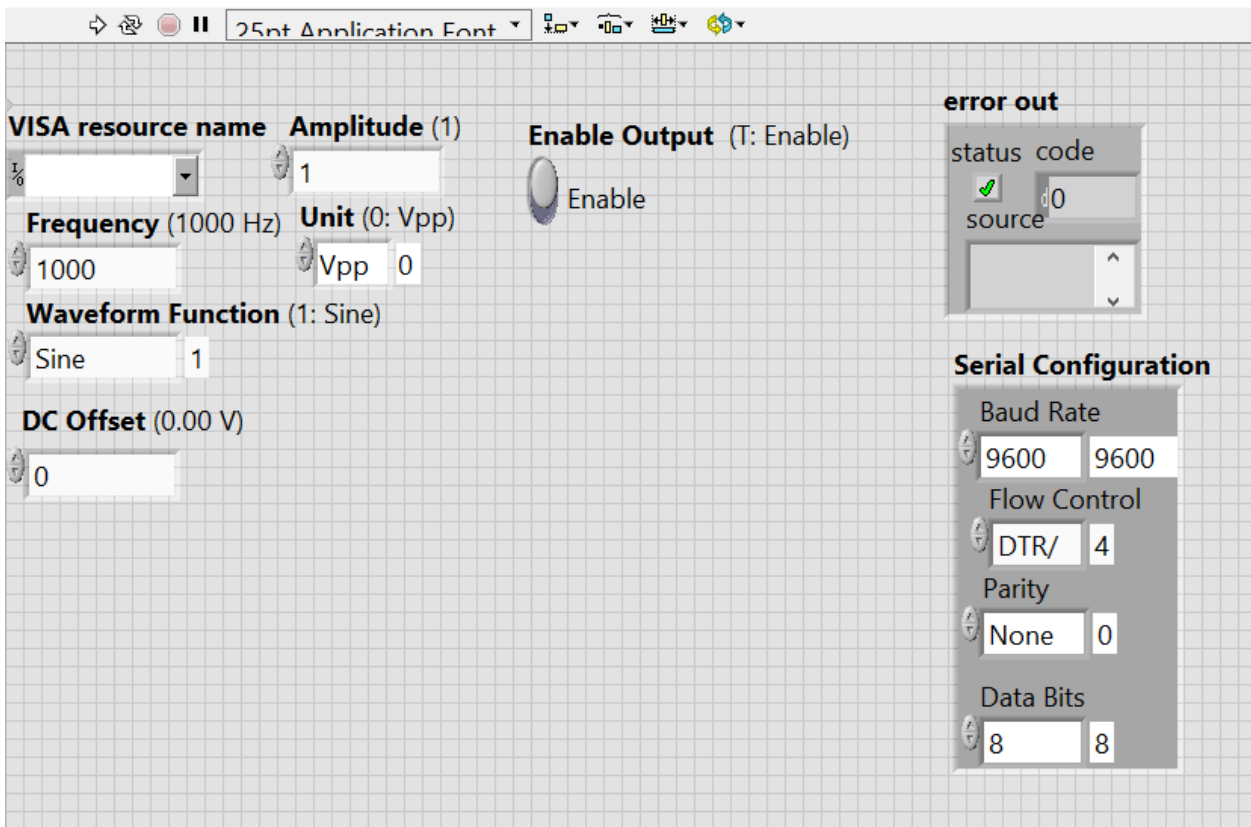


Fig. F-2. Waveform Generator GUI front screen

4. Adjust waveform parameters. After the desired waveform, click the Run button (Arrow) located on the toolbar at the top of the screen. These values should appear on the waveform generator connected to the appropriate PC/Laptop.
5. To output the desired waveform, the Enable Output selection must be toggled. Set waveform parameters -> Press Run -> Stop The Run Instance (Stop Sign) -> Enable Output (toggle button) -> Press Run again. This should result in a continuous output until Stop (Red Stop Sign) is pressed again.

## Agilent DSO-X 2002A Digital Storage Oscilloscope GUI:

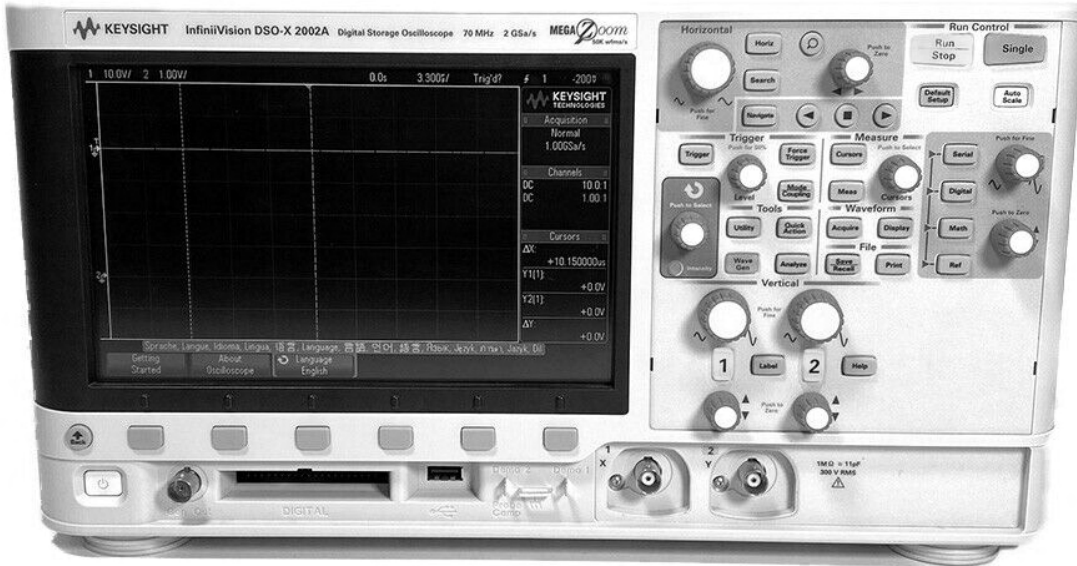


Fig. F-3. Agilent DSO-X 2002A Hardware Front Panel

### Description:

Similar to the waveform generator GUI, this GUI allows the user to remotely control and automate Agilent DSO-X 2002A Digital Storage Oscilloscope via PC/Laptop and a USB connection. The project utilizes this model of Oscilloscope to monitor the pulsing signal of the discharging circuit used to lyse Algae. Specifically, an edge trigger is used to capture the pulse on discharge. This GUI simplifies the Oscilloscopes' many abilities and focuses solely on waveform acquisition based on a trigger edge [21]

### Requirements:

- Agilent DSO-X 2002A Digital Storage Oscilloscope
- USB A to USB B cable connection
- LabView 2021 Application
- GUI Project Files

### Instructions:

1. First connect PC/Laptop to the Waveform Generator using the USB connection cable.
2. Start LabView and open the AlgaeDSO\_GUI.vi Project file.
3. After opening the Project file a simplified version of the Oscilloscope front panel should appear on your screen. (Fig. F-4)

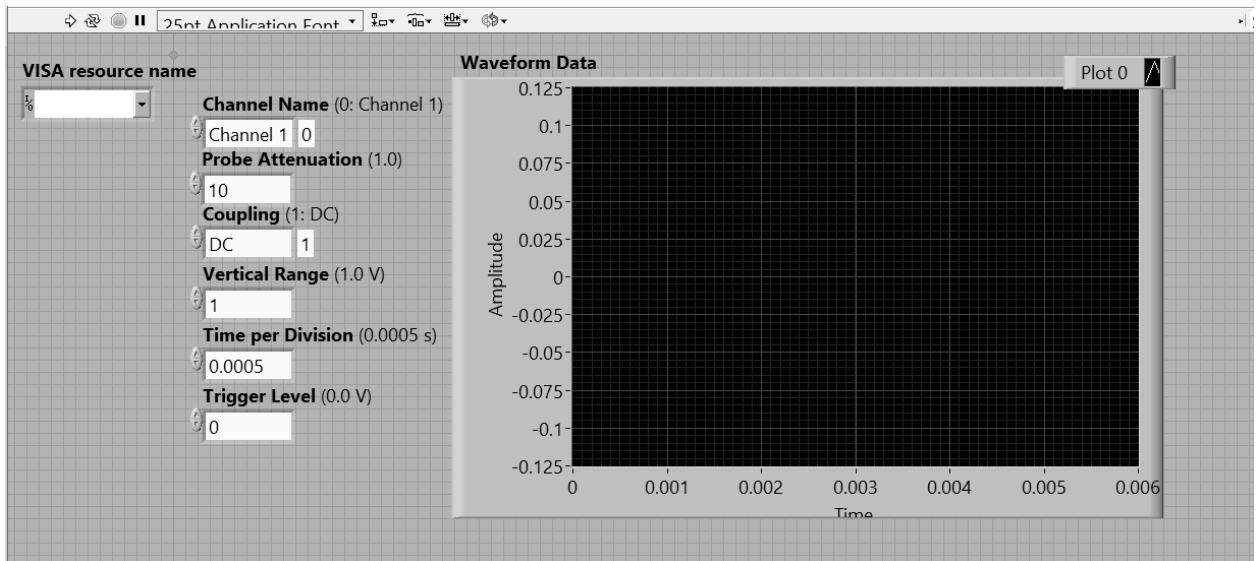


Fig. F-4. Oscilloscope GUI Front Panel

4. Set the desired trigger parameters using the blocks to the left of the waveform graph.
5. After setting the desired trigger parameters, run the application using the Run button (Arrow) located on the toolbar at the top of the screen.
6. The GUI is now active and ready to trigger.

## Appendix E: Digital Multimeter Automation Script

### Description:

This script automates the Voltage Measurement aspect of the multimeter. This simplifies keeping track of the voltage across the discharging capacitor. The voltage taken by the digital multimeter is continuously shown on the console as well as written to a separate, time stamped, text file that can be viewed at the user's discretion. This code works specifically with Rigol Model Digital Multimeters, meaning other multimeters won't work with this code. [22], [23]

### Python Code:

```
import pyvisa
import time
import os

#Data File Creation
dateString = time.strftime("%Y-%m-%d_%H%M")
filepath = "./" + dateString + ".csv"

# This code is assuming a Rigol Multimeter is being used, other digital multimeters
# will not work with this code.

# Query tool usb connections
rm = pyvisa.ResourceManager()

#Lists All connected devices
print("Resources detected\n{}").format(rm.list_resources())

# Initialize Digital Multimeter, the device ID detected should be put in the quotes
# The ID provided below is an example
DMM = rm.open_resource('USB0::0x1AB1::0x09C4::DM1234567890::INSTR')

# Set Digital Multimeter to DC Voltage mode (init)
DMM.write(':FUNCTION:VOLTage:DC')

#Run test
n = input("Continue (y/n)")
while True:
    if n == 'n':
        break
    else:
        vMeas = float( DMM.query(':MEASure:VOLTage:DC?'))
        print("{} {}".format("Voltage", vMeas), end = "\r")
```

```
# write to file
with open(filepath, "a") as file:
    if os.stat(filepath).st_size == 0: # if empty file, write a nice header
        file.write("Measured [V]\n")
    file.write("{:13.5f}\n".format(vMeas)) # log the data
file.close()
```

## **Appendix F: Senior Project Analysis**

### **Summary of Functional Requirements**

This device is an electroporator used in the process of extracting biofuel from algae samples. Electroporation is the process of applying high voltage electric field pulses to create pores and holes in the membranes of cells. As a result, the electroporator is capable of lysing (breaking) algae cell membranes to acquire the lipids and proteins required for biofuel production. The electroporator functions in a lab setting to generate a pulsed electric field (PEF) that outputs waves at specific intervals and strengths to properly lyse the algae cells. Furthermore, the electroporator features a tunable pulse output to offer reliability across different types of algae or environments.

### **Primary Constraints**

Challenges associated with the development of the electroporator include differences in algal strains and shapes, electric field strength and duration, and lack of a systemized approach/process for obtaining results to determine if lysing is successful or not. Due to the variations presented in different samples of algae, the electroporator system must be tunable, as each strain may require a different field strength to be lysed. This requires the option to control the E-field magnitude, the pulse width, and the frequency. Other considerations to account for include the algal cell breakdown points. If too high of an E-field is placed across the algae, then the cell may die due to such a large number of perforations occurring. If the E-field intensity is too low, then the algae cell will not reach the critical voltage of perforation. [24] Lastly, to determine whether lysing occurred, we must check the samples using a microscope, and therefore have no physical data about the process that occurred. To improve this design, there would be a way to obtain measurement data and results by utilizing a graphical user interface (GUI) to output a summary of each experimental run.

### **Economic**

The overall lifecycle of developing an algae electroporator includes the eventual production of the lysed algae into biofuel. This aims to create a net-zero carbon emissions cycle in the development and use of biofuel in the transportation sector. In relation to economic impacts, biofuel integration increases human capital based on the rapidly advancing and up-to-date technological changes taking place in the fuel industry. In other words, individuals working towards this effort are some of the first, and as a result the knowledge they gain is highly valuable since it is limited. Working on the newest products always has this benefit as they rely greatly on creativity and technical skill over legacy designs. This allows individuals to gain expertise in modern advancements and changes that directly impact their environment, economy,

and society. This further promotes sustainability as awareness spreads, particularly if the biofuel industry is successful. People required for this task must be excited to work on new designs and should have a background in an engineering, biology, or related field.

In relation to financial capital, money will need to be expended towards research, testing, and development of the electroporator, as well as the costs related towards manufacturing the biofuel. This includes determining a method and location for growing algae cultures and obtaining the lipids from them. All-in-all, one would expect this to be a very expensive undertaking. The real capital of this venture includes the real estate/ land used to establish a manufacturing facility, machines, measurement tools, required technology, and labor. Natural capital consists of the algae and methods in which they are cultured. The point of this process is for the natural resources to be sustainable and reusable, which is the case presented here. This is in contrast to fossil fuels, which provide no method for replacing the natural resources used to create fuel and result in negative environmental impacts like greenhouse gasses.

Costs for this product accrue primarily throughout the beginning stages of the life cycle. Upfront costs are required to establish a facility and the tools needed for the electroporation system and for production, however the end life and use of the biofuel should generate no harmful effects or costs. In the scope of this senior project and the time allotted in EE 460-462, the costs and development of the electroporator will not be as large-scale as a company fully invested in the production of a sustainable algae biofuel. This senior project is funded by Boeing. The estimated costs for developing the initial electroporator is \$146.6 for materials required that are not already purchased. Test equipment purchased in previous years, such as an impedance analyzer and power supply, are not included in the predicted cost listed above.

### **If manufactured on a commercial basis:**

Despite the end-goal of this project being the production of algae biofuel, and not singularly the electroporator, this manufacturing analysis assumes that the end-product is the electroporator. This is due to the fact that the resources related to costs are more well-known and specific for just the electroporation device. Assuming the electroporator is to be implemented by companies researching the production of biofuels, or trying to extract lipids from similar cells, the small scale electroporator device could be marketed.

The estimated number of devices to be sold under the assumption the electroporator is marketed is 50 units. The estimated fixed manufacturing cost for each device is \$147, not including labor. Adjusting for labor costs, the manufacturing cost can be set to \$500. Therefore, a reasonable market price would be \$700 for a 40% increase. This yields a total addressable market of  $50 * (\$700 - \$500) = \$10,000 / \text{year}$ . The TAM, or total addressable market consists of all the users multiplied by the revenue per user. The operating cost for the user accounts for the cost to

power the device and also to obtain algae or other cellular samples to be lysed, and is therefore variable. Accounting only for power, this cost is approximately \$3.60 per month. The wattage of this device is around 2 W. If the user uses this device 4 hours a day, it will consume around 8 Wh. Since PG&E charges \$0.3 per kWh, the customer will pay around \$0.0024 for the operation of this device daily.

## **Environmental**

Environmental impacts of the manufacturing process relate to the materials and electronics required to develop the electroporation system and algae cultivation systems, as well as the outputs of the system. Within the electroporator is the wiring board assembly containing resistors, capacitors, switches, and an arduino that controls the pulsed electric field (PEF) generation of the system. These devices, if mass produced, cause environmental concerns due to the effects of electronic waste, as well as the energy and water needed to keep the production site running. In comparison to the positive effects of algae biofuel versus petroleum fuel however, this method should prove to be more environmentally friendly and sustainable in the long run.

The main upside to using algae as a source for biofuel is its easy cultivation as well as recycling capabilities. Algae only requires sunlight, carbon dioxide, and water to grow. Carbon dioxide is in excess in our environment, and placing algae ponds or cultivation sites near energy manufacturing plants that produce high amounts of CO<sub>2</sub> helps with this. Rather than creating more CO<sub>2</sub>, like petroleum fuel would do, algae takes in CO<sub>2</sub> and outputs oxygen. In addition, the byproducts of algae biofuel production can be used to create fertilizer and feedstock, meaning everything along the lifecycle is able to be used. [25] Compared to other biofuel sources, such as corn, wheat, or soybeans that require high areas of land to produce and take away from our food supplies, biofuel sourced from algaes has very low environmental impact. Implementing this as a fuel source only helps to foster sustainability and reduce the depletion of natural resources such as fossil fuels.

## **Manufacturability**

Challenges in manufacturing include determining a consistent and reliable method of growing the algae. Algae can be produced in both an indoor or outdoor lab setting. In some cases, algae ponds are implemented to create cultures. This has drawbacks as the algae must be regulated within a particular temperature range. As discussed earlier, the electroporator itself must also account for differences in algae strands that require certain parameters to be lysed. This can be accounted for in the design as long as the wiring assembly contains the proper switches, tunable knobs, and tolerances as outlined in the system's engineering specifications table. When manufacturing the electroporation system, proper funding and testing must be implemented to increase reliability of the system's performance over time.

## **Sustainability**

In the present world, increased populations and demand for natural resources is greater than ever. With that, we have increasingly recognized the responsibility of modern society to take care of those resources to promote a healthy and sustainable future. Fossil fuels make up over 80% of the resources needed for everyday transportation and energy, but they introduce pollutants in our atmosphere and produce greenhouse gasses that are detrimental to the environment. [26] Algae biofuel represents this cleaner alternative with a carbon-neutral life cycle. This method of using electrical fields for lipid extraction proves to be a sustainable process over other present biofuels that continue to use an over-abundance of natural resources, hindering sustainability. In addition, biofuels have characteristics of non-toxicity, biodegradability, and extremely low CO<sub>2</sub> emissions [27]. While this method would certainly provide economic gain as biofuel could eventually overtake other fuel sources used to provide energy, it is moreover being sought after as a necessary effort to reduce carbon emissions and contribute to a healthy society, and sustainable environment.

## **Ethical**

One ethical dilemma that arises in all sectors of the electronic industry is the aspect of waste and how waste from large-scale processes are disposed of if they are no longer required. Along with the manufacturing of ICs, PWBs, or other electronics comes their eventual demise in the form of electronic waste. In order to promote sustainability, the life cycle of technology must not generate waste and rather recycle present materials. Unfortunately, very few devices are recycled properly and safely. Instead, approximately 75% go to landfills or substandard recycling centers [28]. When we dispose of electronic waste improperly, we generate heavy metals, especially lead, mercury, and cadmium, that enter water supplies and food sources. Additionally, most electronic waste processes produce organic pollutants including PBDEs and PCBs, both hazardous to humans, especially children [28]. One ethical concern with any project that uses electronic devices is to ensure that those devices are taken care of properly, such that individuals in countries with lower regulations on E-waste are not harmed by our choices.

Another moral dilemma to consider pertains to the societal implications of conventional and emerging technologies, as listed in the IEEE code of ethics. With any emerging technology, such as biofuel, it is the manufacturer's responsibility to ensure safe and reliable testing has occurred before the product can be sold. The safety and well-being of consumers must be the highest priority over economic gain.

## **Health and Safety**

In order to create the electric fields used to pulse the algae samples, a large voltage must be discharged across the algae at consistent time intervals. Measures would need to be put into place warning users and engineers of the use of high voltages. According to OSHA, the Occupational Safety and Health Administration, all voltages above 50 V are considered to be hazardous. Our current electroporator system has pulse requirements of between 90 V - 120 V<sub>DC</sub>. For this reason, engineers testing the system and anybody near the system while power is on, should be trained according to OSHA's high voltage standards. In addition, the buddy system should be used whenever working in a lab to prevent accidents from happening.

Another health risk to consider is the actual testing and regulation of the final biofuel product. With any emerging or new products on the market, there need to be laws enforced to protect the customers from endangering themselves. Particularly when it comes to fuel, a highly combustible gas, precautions regarding individual safety are vital. The specific uses for the fuel and warning signs need to be properly displayed for the end-user. In addition, the end-product should be fully tested and certified before being available for public use.

## **Social and Political**

The direct stakeholders of this project include the Cal Poly EE, Physics, and Biology supervisors and students, while the extended stakeholders include Boeing and the fuel industry. One social issue that arises from this is the impact that a conversion towards biofuel has on consumers. For example, although sustainability and environmental advocates are in support of cutting carbon emissions with the introduction of biofuel, if successful, the integration of biofuel as a petroleum fuel replacement may face backlash from the public. Biofuel would be a carbon-neutral and sustainable alternative, but it is more expensive to produce. This would subsequently result in higher fuel prices, and would not be supported by all individuals. Some of these individuals could even be considered “Nimby’s” (Not In My Back Yard) due to their opposition to certain changes in their community.

In reference to Garrett Hardin's tragedy of the commons, the increasing demand for fuel, energy, and other natural resources has placed us in a situation where nobody benefits. We are all dealing with the climate crisis, which is a modern day example of a tragedy of the commons. In putting self-interests first, we have collectively over-depleted our resources and contributed to global warming, as the environment is reaching a tipping point. This further exemplifies the need for fuel alternatives and how the beneficiaries of such change includes not only the stakeholders listed above, but also the environment.

This may harm the stakeholders addressed as the fuel industry, particularly the petroleum fuel industry. In replacing fossil fuels with biofuels, the economy would shift. This would impact all parties involved in the fuel industry, as well as consumers in the transportation sectors, or any other areas planning to implement more carbon-neutral fuel sources. Furthermore, the political power of the primary stakeholders in industry would increase as they would have more control over market changes. Ultimately, these changes are hard to realistically project without a well-established biofuel already being in production yet.

## **Development**

As this project incorporates the disciplines of biology, physics, and engineering, there are specific tools that all individuals will become acquainted with that are not directly related to their field of study. One example of this is pipetting, where we must use a pipette to measure specific volumes of algae to place between two glass plates to test the electroporator. Another measurement tool is an impedance analyzer, which is fairly straightforward, but is unlike impedance analyzers used in labs or lectures at Cal Poly. Individual research and simulations must also be completed to assist in design and verification. Since the electroporator circuit does not follow a lecture or classroom example, many strategies in the design process will be self-taught, or backed by research.

## **References**

- [1] Chen, Z., Wang, L., Qiu, S., & Ge, S. (2018). “Determination of Microalgal Lipid Content and Fatty Acid for Biofuel Production.” *BioMed research international*, 2018, 1503126. Available: <https://doi.org/10.1155/2018/1503126>
- [2] Balasubramanian S., Allen J. D., Kanitkar A., Boldor D. Oil extraction from *Scenedesmus obliquus* using a continuous microwave system - design, optimization, and quality characterization. *Bioresource Technology*. 2011;102(3):3396–3403. doi: 10.1016/j.biortech.2010.09.119.
- [3] Ferreira A. F., Dias A. P. S., Silva C. M., Costa M. Effect of low frequency ultrasound on microalgae solvent extraction: Analysis of products, energy consumption and emissions. *Algal Research*. 2016;14:9–16. doi: 10.1016/j.algal.2015.12.015.
- [4] Sathish A, Sims RC. Biodiesel from mixed culture algae via a wet lipid extraction procedure. *Bioresour Technol*. 2012;118:643–647. doi:10.1016/j.biortech.2012.05.118
- [5] Zuorro A., Maffei G., Lavecchia R. Optimization of enzyme-assisted lipid extraction from *Nannochloropsis* microalgae. *Journal of the Taiwan Institute of Chemical Engineers*. 2016;67:106–114. doi: 10.1016/j.jtice.2016.08.016.
- [6] Lee A. K., Lewis D. M., Ashman P. J. Disruption of microalgal cells for the extraction of lipids for biofuels: Processes and specific energy requirements. *Biomass & Bioenergy*. 2012;46:89–101. doi: 10.1016/j.biombioe.2012.06.034.
- [7] S. Kar, et al. “Single-cell Electroporation: Current Trends, Applications, and Future Prospects.” *J. Micromech. and Microeng.*, vol. 28, no. 12, Oct. 2018.
- [8] A. Bessler and J. D. Gonzalez. “Pulsed Electric Field System Development for Algae Biofuel Extraction.” Senior Project, Dept. Elect. Eng., CPSU, San Luis Obispo, CA, 2020
- [9] E. B. Aydin and M. K. Sezgintürk, “Indium Tin Oxide (ITO): A promising material in Biosensing Technology,” *TrAC Trends in Analytical Chemistry*, 25-Sep-2017. [Online]. Available:[https://www.sciencedirect.com/science/article/pii/S0165993617301425?casa\\_token=R2peakVGuUsAAAAA%3AYI33L\\_yNN4jY6NFLRdPf5pHxlPVu8QcSdNNGQO1vVy2jR8EpYByvhfISDa6eRn0EdoRbpfxcg](https://www.sciencedirect.com/science/article/pii/S0165993617301425?casa_token=R2peakVGuUsAAAAA%3AYI33L_yNN4jY6NFLRdPf5pHxlPVu8QcSdNNGQO1vVy2jR8EpYByvhfISDa6eRn0EdoRbpfxcg). [Accessed: 03-Jun-2022].
- [10] “6 in. Dial Caliper,” Harbor Freight Tools. [Online]. Available: <https://www.harborfreight.com/6-in-dial-caliper-63730.html>. [Accessed: 10-Jun-2022].

- [11] E. Luengo, S. Condón-Abanto, I. Álvarez, and J. Raso, “Effect of Pulsed Electric Field Treatments on Permeabilization and Extraction of Pigments from *Chlorella vulgaris*,” *The Journal of Membrane Biology*, vol. 247, no. 12, pp. 1269–1277, Jun. 2014.
- [12] K. Flisar, S. H. Meglic, J. Morelj, J. Golob, and D. Miklavcic, “Testing a prototype pulse generator for a continuous flow system and its use for *E. coli* inactivation and microalgae lipid extraction,” *Bioelectrochemistry*, vol. 100, pp. 44–51, Dec. 2014.
- [13] G. Boesch. Viso. Object Detection in 2022: The Definitive Guide Available: <https://viso.ai/deep-learning/object-detection/>
- [14] <https://www.theimaginingsource.com/products/software/end-user-software/ic-capture/>
- [15] J. Redmon, S. Divvala, R. Girshick, A. Farhardi. University of Washington, Allen Institute for AI, Facebook AI Research. You Only Look Once: Unified, Real-Time Object Detection. *arXiv: 1506.02640v5*, 2015. <https://arxiv.org/pdf/1506.02640.pdf>
- [16] G. Jocher, 2022. Ultralytics [yolov5]. Available: <https://github.com/ultralytics/yolov5>
- [17] “YOLOv5,” *YOLOv5 Documentation*. [Online]. Available: <https://docs.ultralytics.com/>
- [18] tzutalin, 2022. [labelImg]. Available: <https://github.com/tzutalin/labelImg>
- [19] COCO128 [COCOtrain2017]. Available: <https://cocodataset.org/#home>
- [20] M. Thoma, Feb 7th 2017. Available: <https://datascience.stackexchange.com/questions/16797>
- [21] Agilent Technologies, Inc. 2007. Agilent 33220A 20Mhz Waveform Generator. [http://ecelabs.njit.edu/student\\_resources/33220\\_user\\_guide.pdf](http://ecelabs.njit.edu/student_resources/33220_user_guide.pdf)
- [22] Agilent Technologies, Inc. 2011. Agilent InfiniiVision 2000 X-Series Oscilloscopes. User's Guide. [https://www.brown.edu/Departments/Engineering/Courses/En163/2000\\_series\\_users\\_guide.pdf](https://www.brown.edu/Departments/Engineering/Courses/En163/2000_series_users_guide.pdf)
- [23] Michael. “Automating Test-Equipment with Python - Tutorial Australia.” *Core Electronics*, 24 Sept. 2021, <https://core-electronics.com.au/guides/automating-test-equipment-with-python/>.

- [24] Rigol Technologies, Inc. 2014. Rigol Programming Guide.  
[https://www.batronix.com/files/Rigol/Oszilloskope/\\_DS&MSO1000Z/MSO\\_DS1000Z\\_ProgrammingGuide\\_EN.pdf](https://www.batronix.com/files/Rigol/Oszilloskope/_DS&MSO1000Z/MSO_DS1000Z_ProgrammingGuide_EN.pdf)
- [25] (PDF) Electroporation Procedures for Genetic Modification of Green Algae (Chlorella spp.)  
[https://www.researchgate.net/publication/335503044\\_Electroporation\\_Procedures\\_for\\_Genetic\\_Modification\\_of\\_Green\\_Algae\\_Chlorella\\_spp](https://www.researchgate.net/publication/335503044_Electroporation_Procedures_for_Genetic_Modification_of_Green_Algae_Chlorella_spp)
- [26] What Makes Biodiesel From Algae So Exciting? | HowStuffWorks  
<https://science.howstuffworks.com/environmental/green-science/algae-biodiesel1.htm>
- [27] Conversion of residues and by-products from the biodiesel industry into value-added products - Bioresources and Bioprocessing  
<https://bioresourcesbioprocessing.springeropen.com/articles/10.1186/s40643-016-0100-1>
- [28] A critical review on life cycle analysis of algae biodiesel: current challenges and future prospects <https://www.sciencedirect.com/science/article/pii/S1364032120304342>
- [29] Kawahara, Takayuki, and Hiroyuki Mizuno [Eds.] Green Computing with Emerging Memory: Low Power Computation for Social Innovation. Springer, New York, 2013.  
[https://doi.org/10.1007/978-1-4614-0812-3\\_7](https://doi.org/10.1007/978-1-4614-0812-3_7)

## **Group Contribution**

- High Side Switching Bootstrapped Capacitive Circuit
  - Qiying
- Low Side Switching Capacitive Circuit
  - Qiying + Xander
- Inductive Circuit
  - Xander
- Senior Project Analysis (Appendix C)
  - Ashley
- Algae Chamber Characterization
  - Ashley + Hank
- Algae Classification using Convolutional Neural Network
  - Hank
- Graphical User Interface (GUI) and Script for Simplified Data Acquisition
  - Yoel

